

AUTOMOTIVE REAR-END CRASH SIMULATIONS ACCORDING TO FMVSS 310R FOR
EVALUATION OF STRUCTURAL DAMAGE AND PREDICTION OF OCCUPANT
POTENTIAL INJURIES THROUGH LINEAR REGRESSION

A Thesis by

Rithvik Vedantam

Bachelor of Technology, Jawaharlal Nehru Technological University Hyderabad, 2016

Submitted to the Department of Mechanical Engineering
and the faculty of the Graduate School of
Wichita State University
in partial fulfillment of
the requirements for the degree of
Master of Science

December 2018

© Copyright 2018 by Rithvik Vedantam

All Rights Reserved

AUTOMOTIVE REAR-END CRASH SIMULATIONS ACCORDING TO FMVSS 310R FOR
EVALUATION OF STRUCTURAL DAMAGE AND PREDICTION OF OCCUPANT
POTENTIAL INJURIES THROUGH LINEAR REGRESSION

The following faculty members have examined the final copy of this thesis for form and content and recommend that it be accepted in partial fulfillment of the requirement for the degree of Master of Science, with a major in Mechanical Engineering.

Hamid Lankarani, Committee Chair

Krishna Krishnan, Committee Member

Sindhu Preetham Burugupally, Committee Member

DEDICATION

*To My Loving Family, Friends
and
To my advisor, Dr. Hamid M. Lankarani*

Vasudeva sutam devam, Kamsa Chanoora mardhanam/

Devaki paramaanandam, Krishnam Vande Jagad Gurum//

{ I bow to Lord Krishna, the son of Vasudeva, who was the cause of mother Devaki's immense happiness, the destroyer of Kamsa and Chanoora, and who is the supreme teacher of the universe. }

- *Gita Dhyanam (Bhagavad Gita)*

ACKNOWLEDGMENTS

The completion my thesis work has been very challenging yet rewarding, as it would have not been possible to do so without the contribution of several people. I would like to take this opportunity to thank each one of them for their continuous support throughout my journey.

I would first like to thank my advisor, Dr. Hamid M. Lankarani, for his support and for believing in me at times even I could not keep up with all the work. The encouragement and patience are what drove me to the end.

I would also like to sincerely thank my committee members Dr. Krishna Krishnan and Dr. Sindhu Preetham Burugupally, for being part of my committee, and reviewing my thesis report.

I extend my gratitude to my grandparents, parents, in-laws, and family members for their continuous love and support in every step of my life. I would have achieved nothing without my father's guidance and my mother's love.

Finally, I would like to thank the LUNATICS, Thunder Buddies, and all my roommates who made my stay in Wichita feel home, and who were directly or indirectly involved in the completion of my thesis work.

ABSTRACT

The automotive industry has been constantly working to improve the safety of the passengers in cars by researching and upgrading the various features already in use. Although the frequency of rear-end collisions stands third among all the other types, the injuries sustained by the occupants are about one third. This indicates the need for improvement in vehicle crashworthiness and occupant protection during various rear-end collisions. Federal Motor Vehicle Safety Standards (FMVSS), which are issued by the National Highway Traffic Safety Administration (NHTSA), includes some regulations concerning rear impacts, but they essentially cover the vehicle structural responses rather than the potential injuries to the passenger. Therefore, research is needed directed toward enhancing passenger safety during car rear impacts.

The objective of this research is to investigate the structural responses of the car itself and the potential injuries sustained by the passenger in the event of a rear-end collision. Correlation between the structural damage (in terms of interior intrusion, exterior intrusion, and seat acceleration), and the occupant responses (in terms of neck loads and neck moment) are examined using linear regression. LS-DYNA simulations were performed three different classes of cars, according to FMVSS 301R standards for fuel tank integrity in rear-impacts to achieve this. This is done first without the occupant and then with the occupant to compare the injuries sustained by the occupant and to predict the injuries just by examining the crash test structural response. Also, the crash test simulations are conducted on other similar cars to verify these predictions. The results of this study indicate that utilizing this methodology, the potential injuries to the occupants in car rear-impacts can be predicted for the car models for which seats may not be installed.

TABLE OF CONTENTS

Chapter	Page
1 INTRODUCTION.....	1
1.1 Background	1
1.2 Vehicle Crashworthiness and Occupant Safety	1
1.3 Rear-End Collisions	3
1.4 Structural Damage and Injuries Associated with Rear-end Collisions	5
1.5 Injury Mechanisms.....	8
1.6 Injury Criteria.....	10
1.7 NHTSA and FMVSS Regulations	12
1.8 FMVSS 301R Regulation	14
1.9 Research Motivation	15
1.10 Literature Review	16
1.10.1 Vehicle Structural Modifications.....	17
1.10.2 Vehicle Interior Modification and Restraints	17
1.10.3 Occupant Injury Studies	18
2 OBJECTIVES AND METHODOLOGY.....	21
2.1 Objectives.....	21
2.2 General Methodology.....	21
2.3 Computer Aided Engineering (CAE) Tools.....	22
2.3.1 CATIA V5	23
2.3.2 HyperWorks.....	23
2.3.3 LS-PREPOST	24
2.3.4 LS-Dyna.....	24
3 MODELING PROCEDURE.....	25
3.1 Finite Element (FE) Car Models	25
3.1.1 Toyota Yaris	25
3.1.2 Toyota Camry	27

TABLE OF CONTENTS (continued)

Chapter	Page
3.1.3 Ford Explorer.....	29
3.2 Moving Deformable Barrier (MDB, FMVSS 301R)	30
3.3 Hybrid III 50 th Percentile Male Dummy	31
3.4 Rear-End Crash Scenario Modeling.....	33
4 STRUCTURAL RESPONSES OF THE REAR-IMPACT SIMULATIONS	37
4.1 Structural Response of Compact Car (Toyota Yaris).....	37
4.2 Structural Response of Sedan (Toyota Camry).....	40
4.3 Structural Response of SUV (Ford Explorer)	43
4.4 Summary of Structural Responses	46
5 OCCUPANT RESPONSES OF REAR IMPACT SIMULATIONS	47
5.1 Occupant Responses in Compact Car (Toyota Yaris).....	47
5.2 Occupant Responses in Sedan (Toyota Camry).....	49
5.3 Occupant Responses in SUV (Ford Explorer)	52
5.4 Summary of Occupant Injury Responses	53
6 LINEAR REGRESSION OF STRUCTURAL AND OCCUPANT RESPONSES FOR PREDICTION OF INJURIES	55
6.1 Linear Regression of Simulation Results	55
6.1.1 Neck Axial Tension Load.....	56
6.1.2 Neck Extension Moment	57
6.1.3 Neck Longitudinal Shear Force	59
6.1.4 Combined Loading (N _{TE}).....	61
6.1.5 Prediction using Linear Regression	62
6.2 Rear-Impact Test Simulations of Additional Cars for Injury Prediction	63
6.2.1 Dodge Neon	64
6.2.2 Ford Taurus.....	65

TABLE OF CONTENTS (continued)

Chapter	Page
6.2.3 Dodge Caravan	66
6.2.4 Structural Responses of Additional Cars after Rear-end Crash Simulation.	67
7 CONCLUSIONS AND RECOMMENDATIONS.....	72
7.1 Conclusions	72
7.2 Recommendations	74
REFERENCES.....	75

LIST OF TABLES

Table	Page
1.1 Injury Distribution Based on Collision Type and Body Parts (SWOV, 1982).....	7
1.2 Abbreviated Injury Scaling (AIS) (AAAM, 2018).....	8
1.3 Critical Injury Values (NHTSA,2013).....	12
3.1 Toyota Yaris FE Model Summary (NCAC, 2012).....	26
3.2 Actual Vehicle to FE Model Differences (Marzougui, 2012).....	27
3.3 Toyota Camry FE Model Summary (Center for Collision Safety and Analysis, 2016).....	28
3.4 Actual Vehicle to FE Model Differences (Center for Collision Safety and Analysis, 2016).....	29
3.5 Ford Explorer FE Model Summary (Marzougui, 2012).....	30
3.6 FMVSS 301R MDB FE Model Summary (Livermore Software Technology Corporation, n.d.).....	31
3.7 Hybrid III 50th % Model Summary (Livermore Software Technology Corporation, n.d.).....	32
4.1 Structural Responses for FMVSS 301R.....	46
5.1 Occupant Injuries.....	54
6.1 Predicted Injuries.....	63
6.2 Dodge Neon FE Model Summary (National Crash Analysis Center, 2006).....	65
6.3 Ford Taurus FE Model Summary (Marzougui, 2012).....	66
6.4 Dodge Caravan FE Model Summary (National Crash Analysis Center, 2007).....	67
6.5 Structural Responses of the Additional Cars.....	70
6.6 Predicted Occupant Injuries for the Additional Cars.....	71

LIST OF FIGURES

Figure	Page
1.1 Vehicle Chassis (Leiss, 2014).....	2
1.2 Front Frame Rail Tip of a Chevrolet Colorado (Leiss, 2014).....	3
1.3 Number of the Injured Occupant Based on Collision Type (NHTSA, 2016).....	4
1.4 Typical Rear-Crash Causes (Pennsylvania Department of Transportation, 2014).....	5
1.5 Hyper-Extension and Flexion of Neck During Rear-Crash (Mats Y, et al., 2000).....	6
1.6 Various Loadings on the Cervical Spine (Atkinson,2001).....	8
1.7 Hyper-Flexion of the Neck in Frontal Collisions (Murphy, 2009).....	9
1.8 Hyper-Extension of Neck in Rear-Crash (Nevada Department of Public Safety, 2009).....	10
1.9 Car Safety Regulations (Tybout, Fahey, & Crowe, 14 August 2017).....	13
1.10 FMVSS 301R New Regulation (US Department of Transportation, 2007).....	15
1.11 Rear-Crash Distribution (NHTSA, 2015).....	16
2.1 General Methodology of This Research.....	22
3.1 Actual and FE Model of a Toyota Yaris (Marzougui, 2012).....	25
3.2 Interior Components of a Toyota Yaris (NCAC,2012).....	26
3.3 Actual and FE Model of a Toyota Camry (Center for Collision Safety and Analysis, 2016)	27
3.4 Interior Details of Camry FE Model (Center for Collision Safety and Analysis, 2016).....	28
3.5 FE Model of a 2003 Ford Explorer (Marzougui, 2012).....	29
3.6 Ford Explorer Interior View (Marzougui, 2012).....	30
3.7 FE Model of a Moving Deformable Barrier (MDB).....	31
3.8 Hybrid III 50th % Male FE Dummy.....	32
3.9 FMVSS 301 Test Setup with Toyota Yaris.....	33

LIST OF FIGURES (continued)

Figure	Page
3.10 FMVSS 301 Test Setup with Toyota Camry	33
3.11 FMVSS 301 Test Setup with Ford Explorer.....	34
3.12 Toyota Yaris Simulation at $t = \{0,5,10,15\}$ ms	35
3.13 Toyota Camry Simulation at $t = \{0,5,10,15\}$ ms.....	35
3.14 Ford Explorer Simulation at $t = \{0,5,10,15\}$ ms.....	36
4.1 Toyota Yaris Before the Crash	37
4.2 Toyota Yaris After the Crash.....	37
4.3 Overall Length of Toyota Yaris at $t=0$ ms	38
4.4 Overall Length of Toyota Yaris at $t=1$ ms	38
4.5 Cabin Length of Toyota Yaris at $t=0$ ms	39
4.6 Cabin Length of Toyota Yaris at $t=15$ ms	39
4.7 Seat Acceleration Plot for Yaris	40
4.8 Toyota Camry Before the Crash	40
4.9 Toyota Camry After the Crash.....	41
4.10 Overall Length of Toyota Camry at $t=0$ ms.....	41
4.11 Overall Length of Toyota Camry at $t=9$ ms.....	41
4.12 Cabin Length of Toyota Camry at $t=0$ ms	42
4.13 Cabin Length of Toyota Camry at $t=9$ ms	42
4.14 Seat Acceleration Plot for Camry	43
4.15 Ford Explorer Before the crash.....	43
4.16 Ford Explorer After the crash	44

LIST OF FIGURES (continued)

Figure	Page
4.17 Overall Length of Explorer to t=0ms.....	44
4.18 Overall Length of Explorer at t=9ms.....	44
4.19 Cabin Length of Explorer at t=0ms	45
4.20 Cabin Length of Explorer at t=11ms	45
4.21 Seat Acceleration Plot for Explorer	46
5.1 Occupant Responses in Toyota Yaris	48
5.2 Occupant Responses in Toyota Camry.....	50
5.3 Occupant Responses in Ford Explorer.....	52
6.1 Neck Tension Load vs Exterior Intrusion.....	56
6.2 Neck Tension Load vs Interior Intrusion.....	56
6.3 Neck Tension Load vs Seat Acceleration.....	57
6.4 Neck Extension Moment vs Exterior Intrusion	58
6.5 Neck Extension Moment vs Interior Intrusion.....	58
6.6 Neck Extension Moment vs Seat Acceleration.....	59
6.7 Neck Longitudinal Force vs Exterior Intrusion	60
6.8 Neck Longitudinal Force vs Interior Intrusion	60
6.9 Neck Longitudinal Force vs Seat Acceleration	61
6.10 N _{ij} vs Exterior Intrusion	61
6.11 N _{ij} vs Interior Intrusion	62
6.12 N _{ij} vs Seat Acceleration.....	62
6.13 FE Model of a 1996 Dodge Neon (National Crash Analysis Center, 2006).....	64

LIST OF FIGURES (continued)

Figure	Page
6.14 Dodge Neon FE Model Interior View (National Crash Analysis Center, 2006).....	64
6.15 FE Model of 2001 Ford Taurus	65
6.16 FE Model of 1997 Dodge Caravan	66
6.17 Rear-Impact modeling of Dodge Neon.....	67
6.18 Rear-Impact modeling of Ford Taurus	68
6.19 Rear-Impact modeling of Dodge Caravan	68
6.20 Structural Responses of Dodge Neon	69
6.21 Structural Responses of Ford Taurus.....	69
6.22 Structural Responses of Dodge Caravan.....	70

LIST OF ABBREVIATIONS

Abbreviation	Description
AIS	Abbreviated Injury Scale
ATD	Anthropomorphic Test Device
BioRID	Biofidelic Rear Impact Dummy
CAD	Computer-Aided Design
CAE	Computer-Aided Engineering
CAM	Computer Aided Machining
CATIA	Computer Aided Three-Dimensional Interactive Application
DOT	United States Department of Transportation
ES-2RE	EuroSID -2 model with Rib Extensions
Euro NCAP	European New Car Assessment Program
FARS	Fatality Analysis Reporting System
FEM	Finite Element
FEA	Finite Element Analysis
FEM	Finite Element Method
FMVSS	Federal Motor Vehicle Safety Standards
HIC	Head Injury Criteria
IIHS	Insurance Institute for Highway Safety
IPR	Injury Priority Rating
MADYMO	Mathematical Dynamic Model
MATLAB	Matrix Laboratory
MDB	Moving Deformable Barrier
MPP	Massively Parallel Processing
NASS	National Automotive Sampling System
NCAC	National Crash Analysis Center
NCAP	New Car Assessment Program
NCCSA	National Center for Collision Safety and Analysis
NHTSA	National Highway Traffic Safety Administration
NSC	National Safety Council
RID	Rear Impact Dummy
SAE	Society of Automotive Engineers

CHAPTER 1

INTRODUCTION

1.1 Background

The cars we drive today have been evolving for over a century with significant improvements in design and safety options. As cars are the most common method of transport, additional improvements in structural crashworthiness and occupant protection are constantly sought after. An evaluation from the National Safety Council (NSC) shows that the vehicle fatalities topped over 40,000 in 2016. The NSC also estimated that the property damage was more than \$400 billion in 2017 (National Safety Council (NSC), 2018). According to the 2016 Fatality Analysis Reporting System (FARS), there were 1,977 more fatalities in 2015-2016, reporting a 5.6% increase compared to 2014-2015. Thus, there is a significant need for research on crashworthiness and development of the safety standards and features for automobiles now more than ever.

1.2 Vehicle Crashworthiness and Occupant Safety

The ability of a vehicle to absorb the impact and undergo plastic deformation to reduce the injuries caused to the occupants during a crash is called vehicle “crashworthiness”. In the event of a crash, the vehicle cage, known as a chassis, acts a guard preserving the survival space and dissipating or absorbing the impact. This works in conjunction with other safety systems such as airbags and seatbelts, to further reduce any possible injuries to the occupants in the vehicle (Leiss, 2014). The chassis of a vehicle is not only designed to protect the occupants, but also to maintain the functional characteristics such as fuel efficiency and handling. By selecting and incorporating appropriate materials, the chassis is designed to be both safe and efficient. The chassis consists of structural parts such as frames and doors made with steel, and other hard

materials which are used to absorb the energy of the impact. Figure 1.1 shows how a vehicle chassis looks like, which includes all the different structural components including the pillars, frames, and the energy-absorbing components.

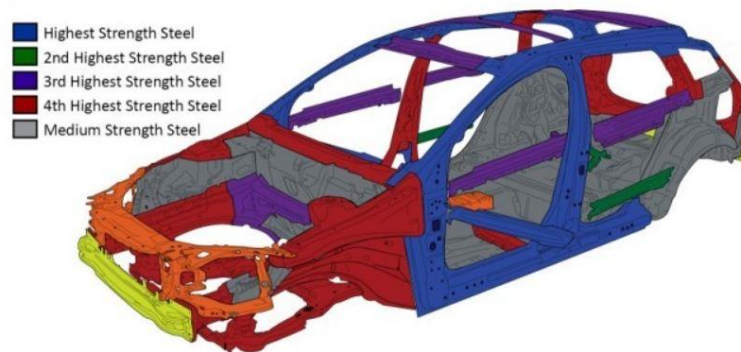


Figure 1.1 Vehicle Chassis (*Leiss, 2014*)

There are different types of vehicle collisions depending upon the crash scenario and impact direction or configuration, namely front, side, rear and roll over. Therefore, the goal of the study of crashworthiness is to:

1. Minimize the crush of the vehicle and maintain the survival space,
2. Prevent ejection from the vehicle during the crash,
3. Dissipate or to completely absorb the crash forces,
4. Prevent post-crash fires.

The crashworthiness safety systems do not prevent the accident itself from happening, rather they minimize the risks of serious injury or death after the accident has occurred. For example, Figure 1.2 is a front frame rail tip on a light truck. The shape and the structure may seem normal to the untrained eye, but the patterned or the ‘rippled’ area is a crush initiation

zone. The patterns on the metal rail create a weak area than the rest of the rails, and hence when there is an accident or an impact, the rail will start collapsing from the rippled area. These initiation zones are carefully designed, checked virtually using FEA, and undergo a series of physical crash tests, thus making the crash a lot less lethal to the passengers.



Figure 1.2 Front Frame Rail Tip of a Chevrolet Colorado (*Leiss, 2014*)

1.3 Rear-end Collisions

A rear-end collision, or simply a rear-end is a car crash scenario in which a vehicle collides with another vehicle in front of it. Rear crashes are the third most frequent type of accidents standing behind the front and side collisions in the United States (NHTSA, 2016). Figure 1.3 shows the total number of persons injured based on the type of collision (NHTSA, 2016).

Breakdown of fatalities and injuries by direction of impact (share and number of persons)

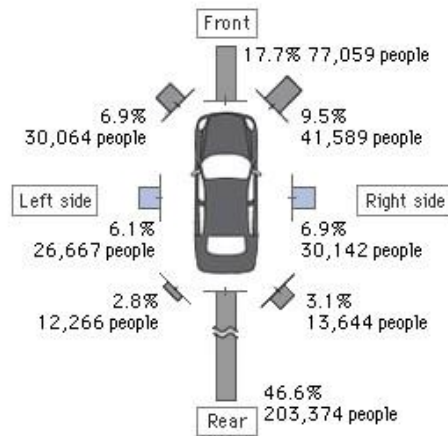


Figure 1.3 Number of the Injured Occupant Based on Collision Type (NHTSA, 2016)

Rear-end collision can be caused by a number of factors. Some of these causes are explained as follows (Sharon Tompkins, 2018):

Tailgating: Tailgating is a violation of the traffic law when a person does not follow the vehicle in front maintaining a safe distance. This makes it impossible for the vehicle to stop in case of an emergency.

Distracted driving: Some of the common distractions in a vehicle while driving are loud music, talking on the phone, texting, eating and operating various instruments. It only takes a few seconds to get distracted and miss a slowing vehicle in front and hit it.

Driver Intoxication: Driving under the influence is a serious problem as it hinders the ability to drive and reduces the reaction time. This would result in misjudgment.

Speeding: The most dangerous rear-end collisions occur during speeding. Judging the space between the vehicles is impossible by a speeding driver. Figure 1.4 shows all the causes for the rear-end collisions (Pennsylvania Department of Transportation, 2014).

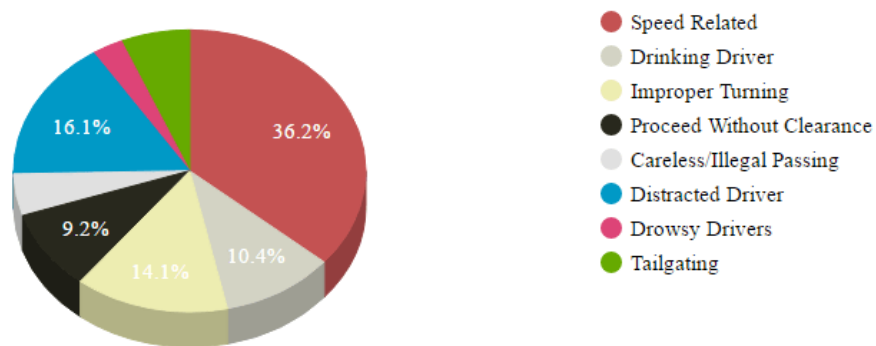


Figure 1.4 Typical Rear-Crash Causes (*Pennsylvania Department of Transportation, 2014*)

1.4 Structural Damage and Injuries Associated with Rear-end Collisions

Structural damage to the vehicle is said to have occurred if any component of a vehicle which is designed to provide structural integrity is deformed due to an impact. Examples of those components include frames (lower rails, upper rails, windshield), bumper, fuel tank, etc.

The most important entity of a car is the frame, on which the entire car is built. The cars today are being built on unibody structures. When a car is struck from the rear, the force of the impact furrows through the car. Aside from the obvious damage which can be seen on the bumper, there could be a structural damage to the frame near any of the wheels. This creates a weak spot on the vehicle, which is susceptible to future damage in the long run.

Consideration of the injuries to the occupants is very important during crashes. Common injuries that people suffer during a rear-end collision include closed head injuries, whiplash and neck injuries, dizziness, and back injuries (compression and extension of discs), (Pike, 1990).

The spine injuries consist of the injuries occurring to the three major parts:

- Lumbar,
- Thoracic,
- Cervical Spine or Neck.

Neck injuries are the most common type of injuries to the occupants in rear-end collision. Thoracic injuries are far less common in rear-end collisions, and so are lumbar injuries. In fact, lumbar injuries occur frequently in aviation accidents. Federal Aviation Regulations (FAR 25.562) (US Department of Transportation, 1992) include a critical tolerance level of 1500lbf (US Department of Transportation, 1992) of load on the lumbar spine.

In a rear-impact, the vehicle is accelerated forward causing the occupant's torso to be pushed forward. The head lags the torso therefore suddenly accelerating and reaching its permissible limit. This neck motion is called an "hyper-extension" and when it protracts, it is called a "flexion". Figure 1.5 shows the mechanism of "hyper-extension" in rear-end collisions.

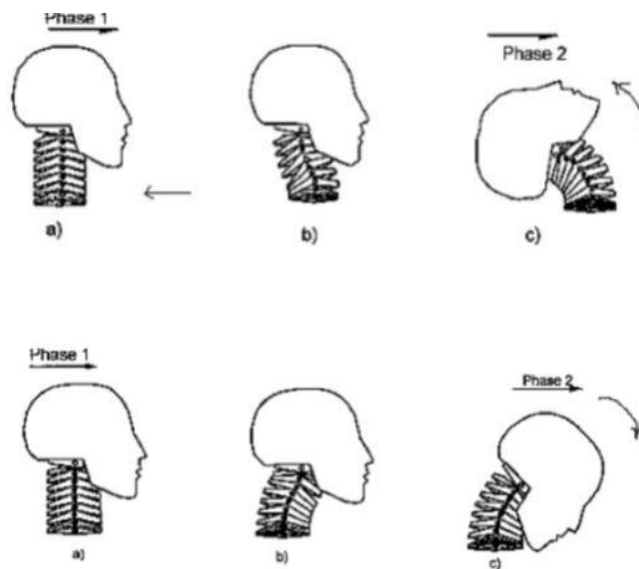


Figure 1.5 Hyper-Extension and Flexion of Neck During a Rear-Crash (*Mats Y, et al., 2000*)

The incidence of neck injuries in traffic accidents appears to be relatively low compared to for instance head injuries, except for specific accident configurations such as rear-end collisions, where more than 50% of the injuries appear to be in the neck area (SWOV, 1982). The distribution of all the injuries to the occupants by body region and also by the accident type are given in Table 1.1:

Table 1.1 Injury Distribution Based on Collision Type and Body Parts (SWOV, 1982)

Main Group	Lateral Collisions	Front to Front	Rear Collisions
1 Skull & Brain	23.7	20.0	14.4
2 Face	11.2	21.1	7.2
3 Neck	4.4	3.7	51.6
4 Thorax	20.2	16.9	6.8
5 Abdomen	2.6	2.3	0.4
6 Back	2.4	1.3	4.0
7 Pelvis	5.0	1.3	0.4
8 Arms	16.0	13.6	7.2
9 Legs	14.5	19.8	8.0
Total	100%	100%	100%

Injury Severity is the severity of the injuries resulting due to the damage experienced by the human body due to impact loading. The anatomic scale which is accepted world-wide which rates the injury itself rather than the consequence of the injury is the Abbreviated Injury Scale (AIS). For example, loss of consciousness and headache injuries are rated as AIS=1. A detailed list of the severity index is given in Table 1.2.

Table 1.2 Abbreviated Injury Scaling (AIS) (AAAM, 2018)

AIS	Severity Code	Injury
0	-	No Injury
1	Minor	Loss of consciousness, Light brain injury, Whiplash, Light cervical spine injuries
2	Moderate	Less than 15-minute unconsciousness, Concussion with or without skull fracture, detachment of the retina.
3	Serious	More than 15-minute unconsciousness without severe neurological damages
4	Severe	More than 12 hours of unconsciousness without hemorrhage in the skull, closed and shifted or impressed skull fracture
5	Critical	More than 12 hours of unconsciousness with hemorrhage in the skull
6	Maximum Injury (Survival not sure)	Death, partly or fully damaged brain stem, spinal cord injury

1.5 Injury Mechanisms

The cervical spine can be loaded in a multitude of different ways (Atkinson, 2001) as shown in Figure 1.6, depending upon the type of collision such as compression, shear and tension forces, bending moment, and torsional force.

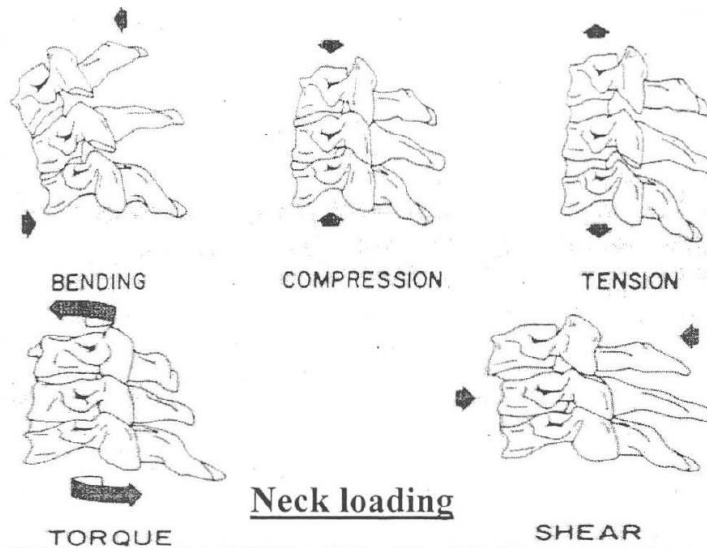


Figure 1.6 Various Loadings on the Cervical Spine (Atkinson, 2001)

Generally, the neck experiences more than one of the above-mentioned forces at the same time during collisions. There are four important categories of neck injury mechanism based on the combined loading on cervical spine:

- Tension-Flexion,
- Tension-Extension,
- Compression-Flexion,
- Compression-Extension.

All these categories arise due to the type of loading on the cervical spine. Tension mechanism has inertial loading of the head playing an important role. The Tension-Flexion mechanism is typically observed in frontal vehicle collisions ($-G_x$ loading) resulting in the hyperflexion of the neck. Figure 1.7 shows the neck motion in a frontal collision. This results in the soft tissue damage to the spine. An exception might be in the case of small children where the head mass is larger in comparison to the strength of the neck which could result in a risk of serious injury.

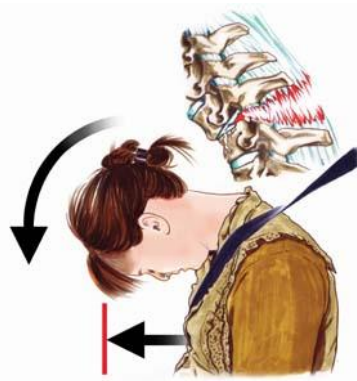


Figure 1.7 Hyper-Flexion of the Neck in Frontal Collisions (*Murphy, 2009*)

The Tension-Extension mechanism is typical for rear-end collisions (+G_x loading). The inertial loading pulls the head backward, resulting in a whiplash when the neck comes into Hyperextension. Figure 1.8 shows the mechanism in rear-end collisions, called the “Hyper-extension”.

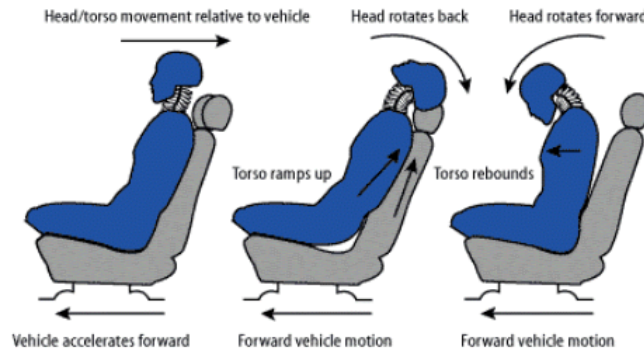


Figure 1.8 Hyper-Extension of Neck in Rear-Crash (*Nevada Department of Public Safety, 2009*)

The compression-flexion mechanism can result in several types of fracture of the vertebral body (wedging and bursting fractures). Also, dislocations, locked facets, and torn posterior ligaments may be a result of this injury mechanism. Damage of the cord is likely in this latter case as well. And finally, Compression-Extension mechanism can cause fractures of the neural arch ligaments (including spinous process) of one or more vertebrae (Lankarani, 2017).

1.6 Injury Criteria

Injury criterion is a measure of the likelihood for an injury to happen to the said body part. Major examples include the Head Injury Criterion (HIC) and Neck Injury Criterion (NIC). The biomechanical response of the cervical spine gives us some information on its tolerance from which, we can deduce the injury criteria. Data gathered by Mertz and Patrick (Mertz &

Patrick, 1971), from their dynamic cadaver tests and accident reconstruction propose tolerance levels for the occipital condyle force and torque levels.

NIC can also be measured based on the combination of linear loads and moments on the cervical spine which was suggested by Prasad and Daniel (Prasad & Daniel, 1984). It is indicated by N_{ij} , where i & j represent the indices of the four injury mechanisms. The first index represents the axial load (tension or compression) while the second index represents the sagittal plane bending moment (flexion or extension). Therefore, when measuring neck injury, each of the following injury criteria shall be met:

The shear force, axial force, and bending moment shall be measured by the dummy upper neck load cell for the duration of the crash event. Shear force, axial force, and bending moment shall be filtered for the N_{ij} purpose at SAE J211/1rev. Mar 95 Channel Frequency class 600 (SAE, 1995)

1) During the event, the axial force (F_Z) can be either in tension or compression while the occipital condyle bending moment (M_Y) can be in either flexion or extension. This results in four possible loading conditions for N_{ij} : Tension-Extension (N_{TE}), Tension-Flexion (N_{TF}), Compression-Extension (N_{CE}), or Compression-Flexion (N_{CF}). (Lankarani, 2017)

2) Critical values of axial force in compression and tension as well as flexion moment when calculating N_{ij} are:

- i. $F_{ZC} = 6806 \text{ N (1530 lbf)}$ when F_Z is in tension
- ii. $F_{ZC} = 6160 \text{ N (1385 lbf)}$ when F_Z is in compression
- iii. $M_{YC} = 310 \text{ Nm (229 lbf-ft)}$ when a flexion moment exists at the occipital condyle

- iv. $M_{YC} = 135 \text{ Nm}$ (100 lbf-ft) when an extension moment exists at the occipital condyle

The linear combination of loads and moments can be expressed in one equation:

$$N_{ij} = F_z / F_{zC} + M_y / M_{yC} \quad (1.1)$$

- F_z is the axial load
- F_{zC} is the critical intercept value of load used for normalization
- M_y is flexion/extension bending moment
- M_{yC} is the critical intercept value for moment used in normalization
- The N_{ij} limit: $N_{ij} < \underline{1.0}$
- It is important to note that the forces and moments are measured concurrent in time for the N_{ij} .

All the peak values for a Hybrid III 50th percentile male dummy are shown in Table 1.3, as per the criteria stated in the federal regulations for assessment of neck injuries.

Table 1.3 Critical Injury Values (*NHTSA,2013*)

Neck Peak Tension (Force)	4170 N
Neck Peak Compression (Force)	4000N
Neck Extension (Moment)	57 Nm
Neck Flexion (Moment)	190 Nm
Neck Shear (Force)	3100 N
N_{ij}	1.0

1.7 NHTSA and FMVSS Regulations

The US Department of Transportation established an agency called as the National Highway Traffic Safety Administration (NHTSA) in 1970, to prevent injuries and reduce vehicle-related crashes thereby saving lives. NHTSA has been constantly monitoring the vehicle

crashes, investigates the causes and has been developing various safety standards which can potentially save lives. It also investigates the defects in vehicle manufacturing and suggests improvements to the vehicle structures and safety features to the manufacturers. There are many regulatory standards that have been issued in the interest of occupant safety. Some of them are (Federal Motor Vehicle Safety Regulations, 2018):

- FMVSS 201 Occupant Protection and Interior Impact
- FMVSS 202a Head Restraints
- FMVSS 208 Frontal Impact Occupant Protection
- FMVSS 214 Side Impact Occupant Protection
- FMVSS 216 Roof Crush Resistance
- FMVSS 223 Rear Impact Guards
- FMVSS 224 Rear Impact Protection
- FMVSS 301 Fuel System Integrity (modified to 301R in 2008)

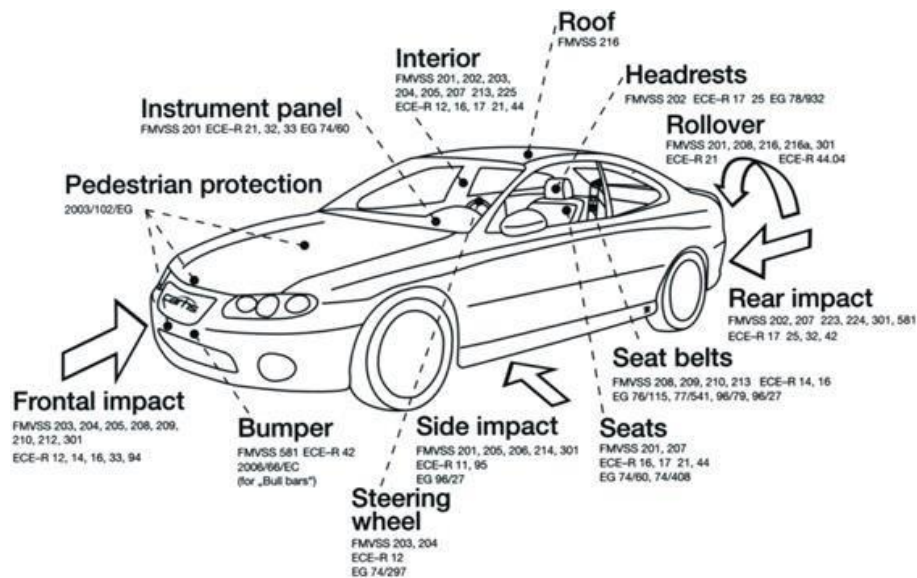


Figure 1.9 Car Safety Regulations (Tybout, Fahey, & Crowe, 14 August 2017)

The United States also initiated the New Car Assessment Program (NCAP) with the primary purpose of giving the customers a measure of the relative safety potential of vehicles in various crashes. This runs under the control of the NHTSA in its facility. Figure 1.9 shows the car safety standards in use in the United States under the FMVSS regulations. All these standards and tests are performed at the NHTSA test facilities under the New Car Assessment Program (NCAP).

1.8 FMVSS 301R Regulation

The NHTSA has a mandate under the legislation, Title 49 of the United State code, Chapter 301, Motor Vehicle Safety, to issue FMVSS a regulation to which the manufacturers should confirm, comply and certify with the standard. These requirements are stated as “the public is protected against the risk of injuries and death in the event of a crash by the design and performance of the vehicle”.

Post-crash fires are rare events but may result in fatalities. According to NHTSA’s Fatality Analysis Reporting System (FARS), from 1991 to 2001, 2.5 to 2.8 percent (NHTSA, 2013) of cases of fatally injured occupants in light vehicles were involved in post-crash fires. NHTSA issued the final rule to upgrade the requirements of the fuel system integrity on December 1, 2003.

The purpose of the FMVSS No. 301 upgrade is to reduce deaths and injuries occurring from post-crash fires that result from fuel spillage during and after motor vehicle crashes and resulting from ingestion of fuels during siphoning (NHTSA, 2014). The rear impact upgrade phased during models 2007 and 2009. From 2007 to 2011, there are about 65 fatalities every year in post-crash, so NHTSA believes that due to upgradation of FMVSS 301 there is estimated that it could save 23 lives per year (NHTSA, 2014).

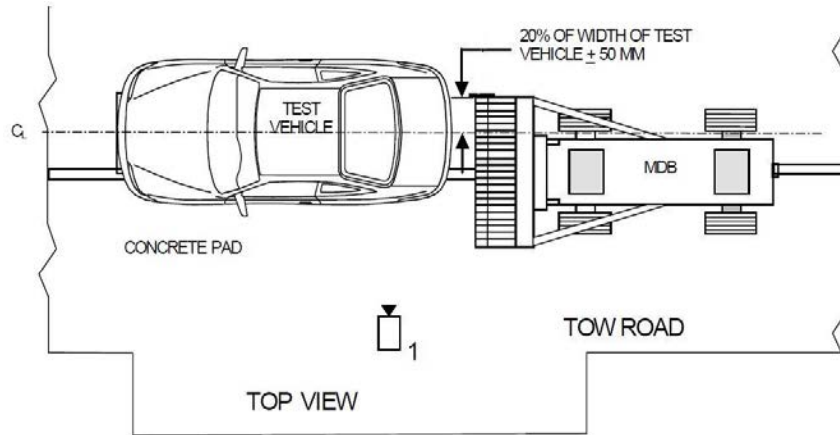


Figure 1.10 FMVSS 301R New Regulation (*US Department of Transportation, 2007*)

In the FMVSS 301R, a moving deformable barrier impacts the rear of the vehicle at 80kmph (~50mph). The regulatory standard setup with the MDB having a 70% overlap to the target vehicle is shown in Figure 1.10.

1.9 Research Motivation

NHTSA issued a rule to upgrade the FMVSS 301 regulation which previously dealt with the fuel system integrity to a new regulation, FMVSS 301R. It still does the same but is more effective in inspection, which in turn reduces the injuries and potential deaths of occupants in the event of a post-crash fire due to the fuel leakage. Though this regulation has been successful in preventing the number post-crash fuel leakages, the effect of a rear-impact on the occupant has not been extensively examined. There exist additional standards, namely FMVSS 224, focusing on the occupant safety in rear-end collision, but these are designed for low-speed rear-impacts, and do not necessarily represent major injury-producing rear-impact scenarios.

Rear-end collisions can occur in four types as shown in Figure 1.11 (NHTSA, 2015). It can be observed that the most occurred rear-end crash is the rear offset collision. Coincidentally,

the FMVSS 301R regulation also uses a similar scenario for the test where the occupant's response can be studied.

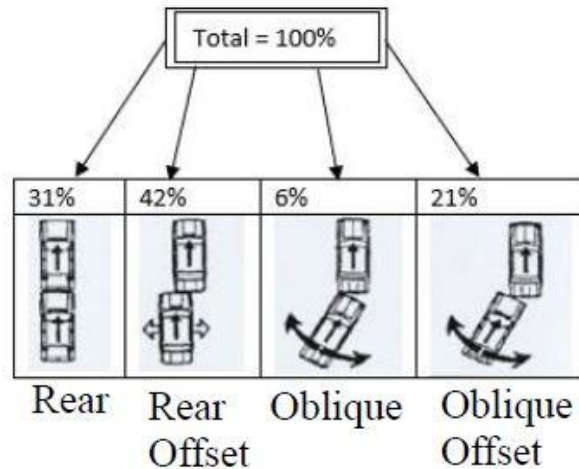


Figure 1.11 Rear-Crash Distribution (NHTSA, 2015)

1.10 Literature Review

Several sources concerning vehicle collisions and, the research papers concentrating on rear-end crashes have been studied to better understand the previous work done on this topic. In general, the literature can be grouped into three categories, namely:

- Rear-end collision vehicle structural modifications
- Rear-end collision vehicle interior modification and restraints
- Rear-end collision occupant injury evaluation

Each of these shall now be discussed individually.

1.10.1 Vehicle Structural Modifications

(Heinrichs, et al., 2001) studied both rear and front collisions for five pickup trucks and compared the collision severity with vehicle to vehicle as well as vehicle to barrier collisions. All the collisions, accelerations and the bumper damages are recorded, and it was shown that there was a significant correlation between barrier and vehicle crash values.

(Martin, 2002) studied the influence of tow-bars in rear-end collision of two cars. Three cases of rear-crashes were studied, and it was concluded that it is not good having an over-ride situation, Under-ride situation resulted in a 'softer' impact, and the addition of a tow-bar in any of the cases resulted in a higher risk of getting neck injuries.

(Atahan, 2003) proposed design modifications to under-ride guard that minimally complies with requirements contained in FMVSS 223/224. A full-scale crash test simulation was performed to show that the modified rear under-ride guard performs much better than the original design.

(Avery, 2006) has concluded that the bumper beam was the key feature in determining the severity of the damage to the vehicle in low-speed rear impacts. The study included two variations at a speed of 15kmph, first with a 40% overlap and a 10° impact and the second one being a 70% overlap with the same angles. It was concluded that the bumper beam and its geometry are crucial in determining the damage severity of the vehicle.

1.10.2 Vehicle Interior Modification and Restraints

(Kleinburger, 1999) did a computational study to better understand the risk to the neck and spine in a rear-impact. The effects of a head restraint were also considered. Due to the unavailability of dummies, a cadaver was used. The study concluded that the increasing the

height of the head restraint by 2.5 inches – 5.5 inches than the average would reduce the loads on the cervical spine during low speed rear-impacts.

(Derosia, 2003) obtained acceleration pulses for 5th, 50th and 95th percentile Hybrid III dummies by performing rear sled tests and evaluated injury criteria. The tests were performed and the N_{ij} values were compared for increasing seat back distance.

(Jagan, 2004) optimized the vehicle interior configurations at a low speed rear-end collision. Acceleration pulse was obtained from the driver seat node and the N_{ij} values of Hybrid III dummy with a variation in seat back angles (9° and 22°) and head restraint positions were taken and examined. The study concluded that a higher seat back angle and better seat cushion properties result in lower whiplash injuries.

(Herbst, 2009) tested different seat designs using Quasistatic Seat Test (QST) methodology on an Anthropometric Test Dummy (ATD) and showed that the load to the seat back through the lumbar spine of the ATD can be a predictor of seat deformation under dynamic loading. Additionally, FMVSS 301R test with ATD was conducted and the degree of encroachment of the deforming seat back onto the rear occupant's seating compartment was analyzed.

(Jugge, 2017) studied the structural damage of a compact car in different possible rear-impact conditions and evaluated the potential injuries to the occupant with and without a head restraint using FMVSS 301R regulations.

1.10.3 Occupant Injury Studies

(Ragland, et al.,1998) studied the effects of rear-end collisions on different vehicles using an FMVSS 214 deformable barrier. The study concentrated on fuel system integrity and fuel

leakage. In conclusion, the head and chest injury values of a Hybrid III anthropomorphic test device (ATD) are validated.

(Kleinburger, et al., 1999) again studied whiplash injuries to the head-neck complex. They provided a brief perspective on the efficiency and importance of the experimental research and used a human cadaver for the research.

(Eriksson & Boström, 1999) studied the major risk factors for whiplash in a rear-end crash namely crash pulse, seat force characteristics, and head restraint position using a BioRID MADYMO dummy model. In addition, a Neck Injury Criterion (NIC) has also been proposed by means of dummy, human and rear-impact simulations.

(Schmitt et al., 2001) developed and proposed a new neck injury predictor called N_{km} . Results from a total of 37 sled tests with various car seat models were evaluated to validate this model. This criterion offers possibility to assess kinematic possibility of forward motion of the neck in rear-end collision.

(Ranganatha, 2003) studied about different neck loads influenced by the various seat back angles during different low-speed crash scenarios on a mid-size sedan. Ford Taurus was hit with a deformable barrier in three different speeds and the acceleration pulse is obtained. Then, parametric neck loads of Rear Impact Dummy and Hybrid III 50th % dummy were observed using MADYMO.

(Butala, 2003) studied neck injuries for Rear Impact Dummy 2 (RID 2) and Biofidelic Rear Impact Dummy II (BIORID II) under various impact conditions. Rear collision, rear offset collision, and rear angled collisions are performed for three different cars with three different speeds. The acceleration pulses obtained, and the responses of the dummies were studied.

(Gunter, et al., 2005) studied on five different collision pulse properties, namely peak acceleration, speed change, duration, displacement and shape during a rear impact collision and their effect on the severity of the whiplash injuries on a BIORID dummy.

(Patel, 2007) studied the “rear impact of light trucks and the potential injuries to the occupant”. Neck injuries for Hybrid III 50th percentile dummy with and without a head restraint. The acceleration pulses were obtained for three different trucks at 5mph, 10mph, and 20mph respectively.

(Amir Hassan, 2005) studied the structural damage as well as occupant injury on a vehicle colliding with a rigid pole and compared them to the same vehicle colliding a flat barrier. It was concluded that the intrusions and injury values were more severe in case of pole impact and there might be a severe leg injury.

(Kuppa, 2006) presented a whiplash injury criterion based on the head-to-torso rotation using hybrid III 50th percentile male dummy in a rear-impact and was able to rank the effectiveness of head restraint/seat systems in FMVSS 202 dynamic option sled tests.

CHAPTER 2

OBJECTIVES AND METHODOLOGY

2.1 Objectives

The goal of this study is to utilize the FMVSS 301R Fuel Systems Integrity as a methodology for the evaluation of the structural damage to the vehicle and the prediction of potential injuries to the occupants in rear-impact collisions. The structural damage to the vehicle and the occupant injuries are correlated through linear regression for injury prediction. The specific objectives identified for this research are:

- To identify three different sized cars, namely a compact car, a sedan, and an SUV, and utilize their finite element (FE) models.
- To reconstruct the FMVSS 301R fuel system integrity test for the above-identified cars, with and without the occupant.
- To extract the maximum car and cabin intrusions along with the maximum seat accelerations after the crash without the occupant.
- To examine occupant injuries from the crash test.
- To correlate the obtained occupant injuries to the structural damage of the cars, using a regression model.
- To perform additional crash test simulations and predict occupant injuries based on the correlations.

2.2 General Methodology

The research work begins with the modeling of the FMVSS 310R rear-impact crash test with three different cars. The cars used for this research are

1. 2010 Toyota Yaris (Compact car)
2. 2012 Toyota Camry (Sedan)
3. 2003 Ford Explorer (Explorer)

The reconstruction of the crash test is simulated for each of these cars with and without the occupant to get the intrusions and accelerations. The results are then correlated and validated with an occupant in the same crash scenario, with different cars. Figure 2.1 depicts the complete methodology carried out in this thesis.

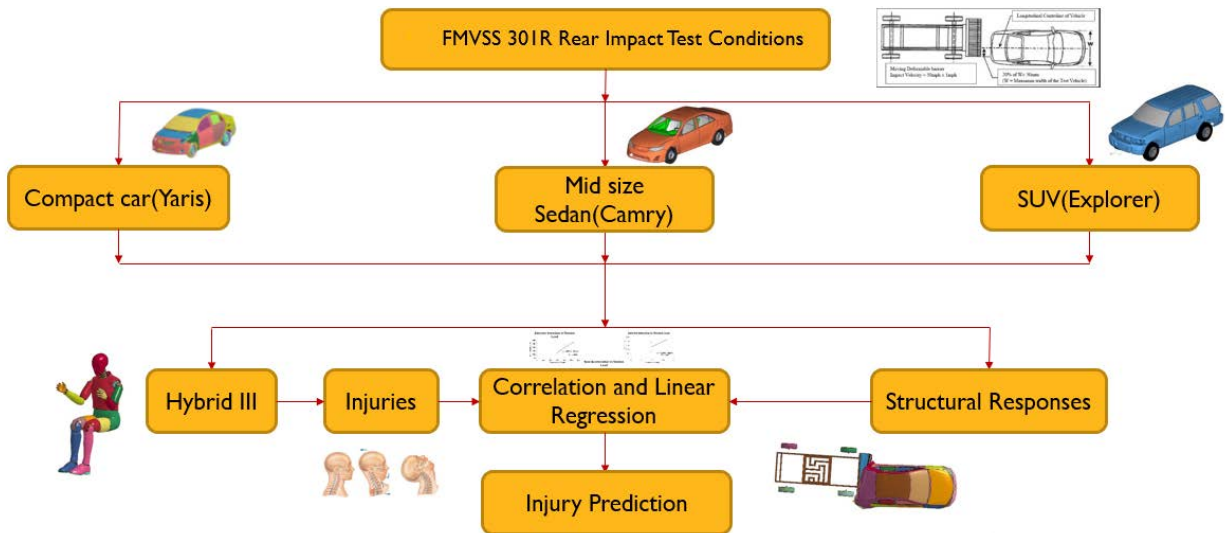


Figure 2.1 General Methodology of This Research

2.3 Computer Aided Engineering (CAE) Tools

The reconstruction of crash tests is an effective way of understanding the scenario but doing it every time takes a lot of time and effort. Production of modern day vehicles has become costly due to they are more sophisticated. Therefore, the development of a multi-purpose crash simulation software is very much necessary.

CAE tools are widely used in both aviation and automotive industries to conduct crash tests. These tools can be used multiple times which improves the safety, strength, and luxury of the people during travel. The progress of CAE has increased in the 21st century and almost all of the crash scenarios can be done effectively in these softwares. The CAE tools used for this research are CATIA V5, Hyperworks, LS-PrePost and LS-Dyna.

2.3.1 CATIA V5

CATIA (Dassault Systemes, 2018) is a multi-platform software suite for computer-aided design (CAD), computer-aided manufacturing (CAM), and computer-aided engineering (CAE). It was developed by the French company Dassault Systèmes. It encourages the genuine cooperative building over the multidisciplinary broadened endeavor, including style from an outline, mechanical plans, hardware plan, and frameworks designing.

2.3.2 HyperWorks

HyperWorks (Altair Engineering, 2014) suite is a complete package of finite element procedure developed by Altair software which includes preprocessing, solving and post-processing. The hypermesh is the finite element analysis tool and is widely used in a variety of CAE tasks like meshing, model check, penetration check, etc. It also acts as a high-performance post processing for solvers like LS-Dyna, Optistruct, and Nastran.

Another great software which comes with HyperWorks is the Hyperview. This software enables the users to visualize the data interactively and also saves the 3-d animation results to share the results in other software platforms like the LS-PrePost, Oasys Primer, and CATIA.

2.3.3 LS-PREPOST

The LS-PrePost (Livermore Software Technology Corporation (LSTC), 2007) is an advanced pre and post-processor that is delivered free with LS-Dyna. The user interface (UI) is designed to be both efficient and intuitive. It uses OpenGL graphics to achieve that fast rendering. Preprocessing features include 2d, surface, solid and tool meshing, dummy positioning and seat belt fitting. D3plot animation, BINOUT processing, and ASCII plotting are some of the important post-processing features of this software. In this research, 70% of the total tool usage is done with LS-PrePost.

2.3.4 LS-Dyna

LS-Dyna (Livermore Software Technology Corporation, 2011) is the solver in which the numerical calculations can be done for static, dynamic, implicit and explicit analysis and solves real-world problems. LS-Dyna is perfect for crashworthiness analysis like automotive and aviation. This software computes on the cluster for solving the problems. LS-Dyna was the primary solver used for this research.

CHAPTER 3

MODELING PROCEDURE

The modeling procedure for the various simulations starts with the Finite Element (FE) models. This chapter gives an overview of all the FE models used to run the simulations during the research.

3.1 Finite Element (FE) Car Models

The research utilizes various Finite Element (FE) Models for the accident reconstruction and simulation of the rear-impact collisions. The models used for this research include 3 cars, one barrier, and a dummy. The details of each model used are discussed below.

3.1.1 Toyota Yaris

The compact car selected for the research is a Toyota Yaris. The Toyota Yaris is an ideal example of a small compact passenger vehicle. The National Crash Analysis Centre (NCAC) has developed a finite element model of a 2010 Toyota Yaris through reverse engineering at the George Washington University (Marzougui, 2012). The isometric view of the car is shown in Figure 3.1:



Figure 3.1 Actual and FE Model of a Toyota Yaris (Marzougui, 2012)

This FE model was reverse engineered by scanning each part and cataloging for accurate geometry and material properties and all the data was input to a computer file and is meshed to create the FE model. Material data for various structures was obtained through coupon testing from the samples taken from the vehicle. Detailed interior of the vehicle is shown in Figure 3.2. The description of the FE model of Toyota Yaris is showed in Table 3.1.



Figure 3.2 Interior Components of a Toyota Yaris (NCAC,2012)

Table 3.1 Toyota Yaris FE Model Summary (NCAC, 2012)

Model	2010 Toyota Yaris
Number of Parts	917
Number of Nodes	1,480,422
Number of Shells	1,250,424
Number of Beams	4,738
Number of Solids	258,887
Total Number of Elements	1,514,068
Beam Element Connections	4,425
Rigid Body Connections	2
Joint Connections	39

The FE model is validated in several ways to ensure that it is as accurate as possible.

Table 3.2 shows the difference in data between the actual vehicle and the FE model.

Table 3.2 Actual Vehicle to FE Model Differences (*Marzougui, 2012*)

	Actual Vehicle	FE Model
Weight, kg	1078	1100
Pitch inertia, kg-m²	1498	1566
Yaw inertia, kg-m²	1647	1739
Roll inertia, kg-m²	388	395
Vehicle CG X, mm	1022	1004
Vehicle CG Y, mm	-8.3	-4.4
Vehicle CG Z, mm	558	569

3.1.2 Toyota Camry

The sedan selected for this research is a 2012 Toyota Camry. The FE model was developed by the Center for Collision Safety and Analysis (CCSA) researchers at the George Mason University (Center for Collision Safety and Analysis, 2016) sponsored by the Federal Highway Administration (FHA). This model was created with LS-Dyna FE software. The actual car and the isometric FE model are shown in Figure 3.3 while the interior details of the FE model are shown in Figure 3.4



Figure 3.3 Actual and FE Model of a 2012 Toyota Camry (*Center for Collision Safety and Analysis, 2016*)



Figure 3.4 Interior Details of Toyota Camry FE Model (*Center for Collision Safety and Analysis, 2016*)

The actual car was purchased, and reverse engineered at the facility and a detailed FE model was developed (*Center for Collision Safety and Analysis, 2016*). The interior details of the FE model of the car are shown in Figure 3.4. The total details concerning the model are shown in Table 3.3.

Table 3.3 Toyota Camry FE Model Summary. (*Center for Collision Safety and Analysis, 2016*)

Model	2012 Toyota Camry
Number of Parts	1,086
Number of Nodes	2,255,361
Number of Shells	2,032,594
Number of Beams	5,901
Number of Solids	218,785
Number of Elements	2,257,280

The model was validated using a series of tests like a general check of the vehicle CG and inertia, then the NCAP frontal wall impact was compared with the actual test. Table 3.4 shows the comparison of the various parameters obtained.

Table 3.4 Actual Vehicle to FE Model Differences (*Center for Collision Safety and Analysis, 2016*)

	Actual Vehicle	FE Model
Weight, kg	1452	1462
Pitch inertia, kg-m²	2519	2524
Yaw inertia, kg-m²	2796	2807
Roll inertia, kg-m²	560	572
Vehicle CG X, mm	1063	1086
Vehicle CG Y, mm	-9	-1
Vehicle CG Z, mm	561	560

3.1.3 Ford Explorer

The SUV used for this research is a Ford Explorer. The FE model was reverse engineered at the George Washington University by the National Crash Analysis Center (NCAC) in 2012 (Marzougui, 2012). The FE isometric model and the detailed interior model are shown in Figures 3.5 and 3.6.

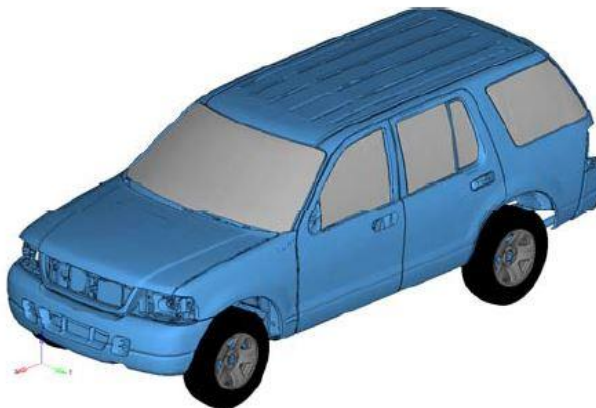


Figure 3.5 FE Model of a 2003 Ford Explorer (*Marzougui, 2012*)

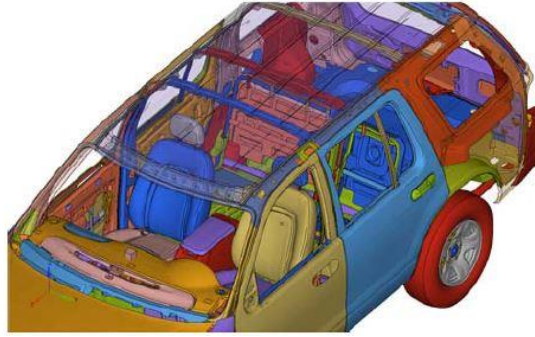


Figure 3.6 Ford Explorer Interior View (*Marzougui, 2012*)

Validation was done in comparison to NCAP frontal test data from NHTSA tests 3730 and 5034 (NHTSA, 2018). The FE model summary is shown in Table 3.5.

Table 3.5 Ford Explorer FE Model Summary (*Marzougui, 2012*)

Model	2003 Ford Explorer
Number of Parts	923
Number of Nodes	724,628
Number of Shells	680,288
Number of Beams	185
Number of Solids	33,690
Number of Elements	714,205

3.2 Moving Deformable Barrier (MDB, FMVSS 301R)

To simulate the rear-end collision, a barrier is also needed as an FE model. Moving Deformable Barriers (MDB) are the most widely used barrier, however, not all the crash tests use the same kind of barrier. The barrier specific to FMVSS 310R is downloaded from LSTC's website (Livermore Software Technology Corporation, 2018). The MDB face assembly has a bumper which is constructed of honeycomb 1690 kPa sandwiched between thick aluminum

plates (Kalaga, 2018). The barrier FE model and the specifications are shown in Figure 3.7 and Table 3.6.

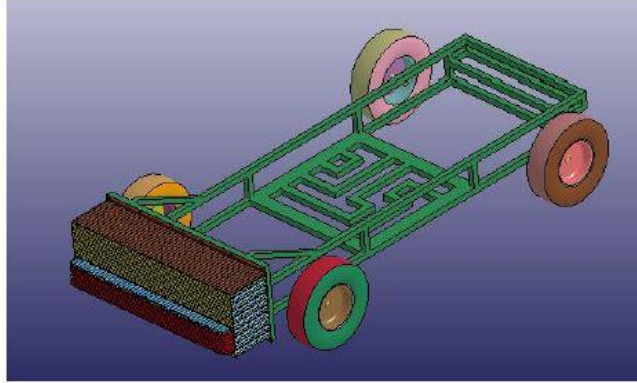


Figure 3.7 FE Model of a Moving Deformable Barrier (MDB)

Table 3.6 FMVSS 301R MDB FE Model Summary (*Livermore Software Technology Corporation, 2018*)

Model	Deformable Barrier
Version	170920_V4.3
Model	LSTC Shell Barrier
Weight, kg	1368
Wheel Base, mm	2591
Total number of Elements	549,509

3.3 Hybrid III 50th Percentile Male Dummy

Livermore Software Technology Corporation developed and validated a variety of dummies including the 50th, 5th, and 5th percentile male and female dummies. All these dummies each have both a rigid and a deformable version. Since these dummies were first released in the '90s a lot of work has been to put into them to further develop and to run them quickly and

robustly and making them useful in solving the real-world problems. The dummy selected for this research is the Hybrid III 50th percentile male dummy (LSTC.NCAC_H3_50th_130528_BETA). The isometric view and the specifications are shown in Figure 3.8 and Table 3.7 respectively.



Figure 3.8 Hybrid III 50th % Male FE Dummy

Table 3.7 Hybrid III 50th % Model Summary (*Livermore Software Technology Corporation, 2018*)

Version	LSTC.NCAC_H3_50 th _130528_BETA
Model	Hybrid III 50 th % Male
Weight, kg	78.86
Total number of Elements	4333

3.4 Rear-End Crash Scenario Modeling

The FE models mentioned above are used for the accident reconstruction of a rear-impact crash. The entire crash test setup was modeled using LS-PrePost and was simulated in LS-Dyna solver for 0.15 seconds with the barrier located almost at the point of contact to reduce simulation time.

The barrier moves with an initial velocity of 79.3 kmph (~50mph) with an offset of ~20% of the maximum width of the vehicle. The FMVSS 301R setups for all the three vehicles are shown in Figures 3.13, 3.14 and 3.15.



Figure 3.9 FMVSS 301 Test Setup with Toyota Yaris

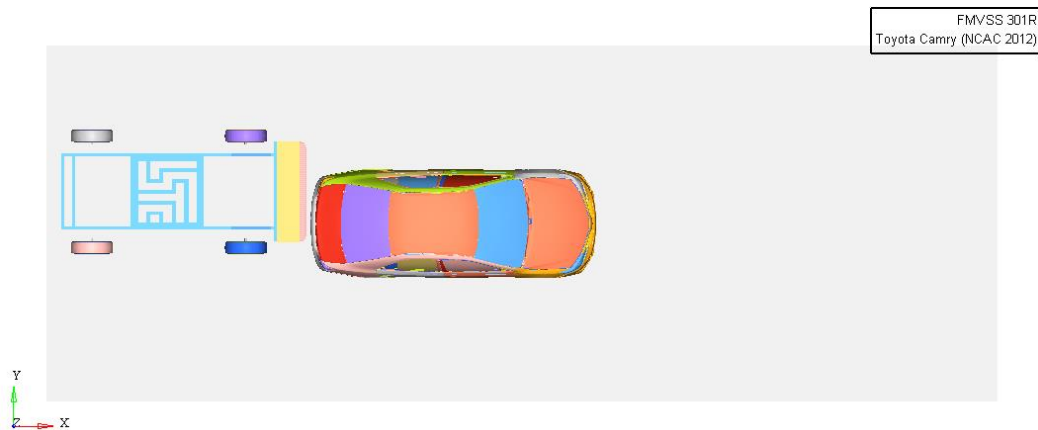


Figure 3.10 FMVSS 301 Test Setup with Toyota Camry

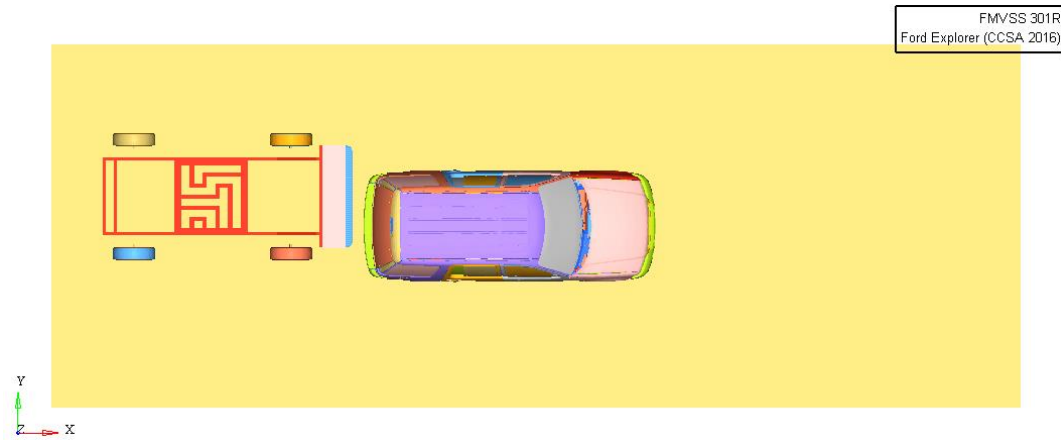


Figure 3.11 FMVSS 301 Test Setup with Ford Explorer

A node set for the entire barrier is created and the input velocity is given using `*VELOCITY_CONTACT` data group in the `*INITIAL` keyword interface. This is used instead of creating a `*SET_PART` to ensure no node is left out while giving the initial velocity to the model.

The contacts among the parts are modeled using a single surface sliding interface `AUTOMATIC_SINGLE_SURFACE` and the contacts between the car and the barrier are given using the keyword `AUTOMATIC_SURFACE_TO_SURFACE`. While giving the contacts, the car, which is a stationary target, is assigned master and the barrier, which is the impactor entity, is assigned as slave.

The termination time has been set to 0.15 seconds in `*CONTROL_TERMINATION` keyword with a time step of $-1.112e^{-6}$ using `*CONTROL_TIMESTEP` keyword. The simulation responses of the cars can be observed in Figure 3.12, 3.13 and 3.14.

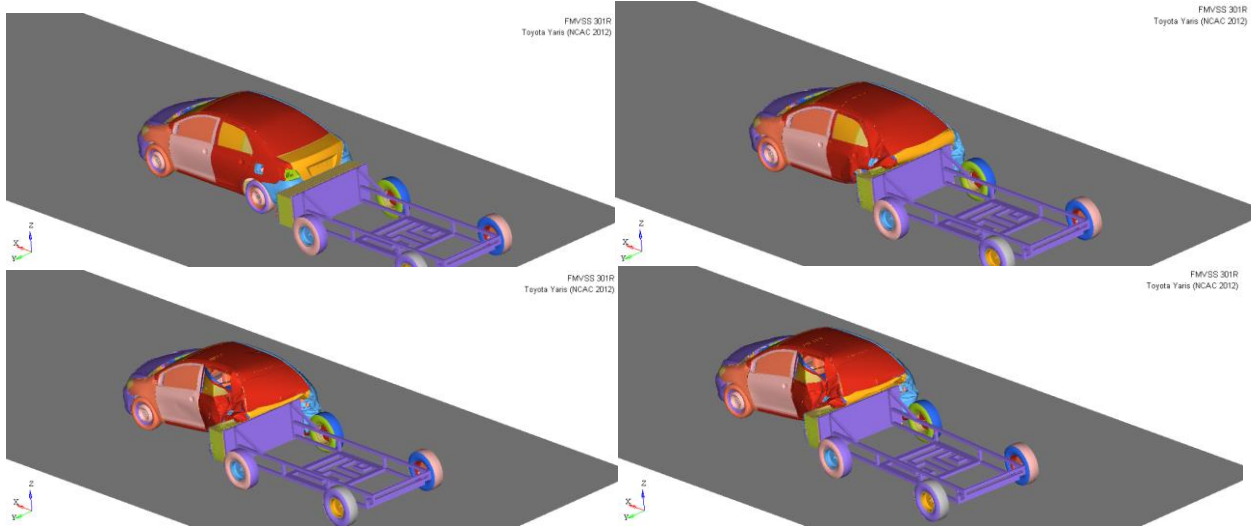


Figure 3.12 Toyota Yaris Simulation at $t = \{0,5,10,15\}$ ms

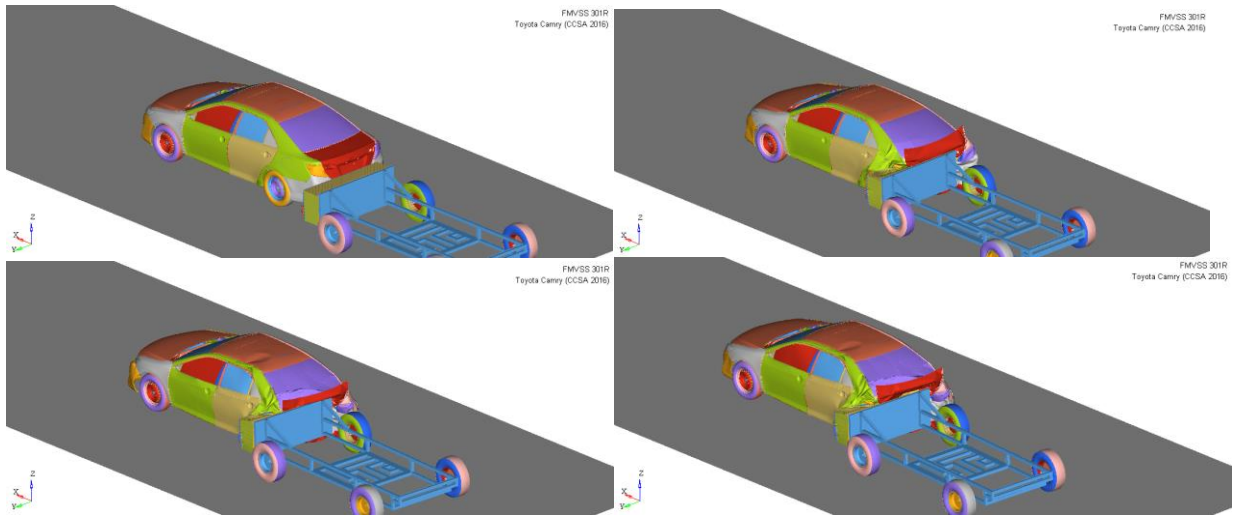


Figure 3.13 Toyota Camry Simulation at $t = \{0,5,10,15\}$ ms

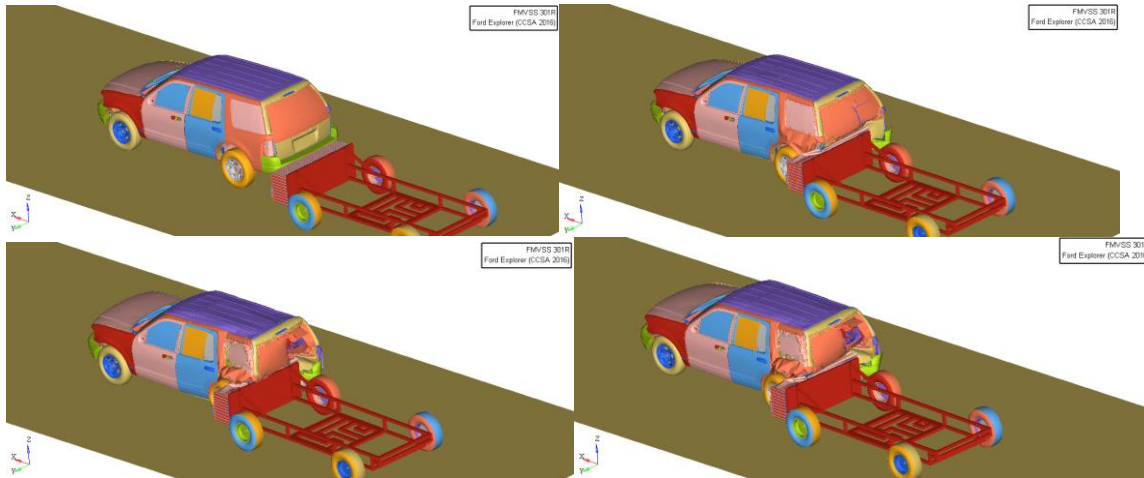


Figure 3.14 Ford Explorer Simulation at $t = \{0,5,10,15\}$ ms

These simulations of the empty vehicle show us that there is a significant damage to the cars. Thus, one can also expect the occupants to be significantly affected by the crash. But before any simulations are done with occupants, the post-processing of the FMVSS 301R tested models is achieved using the LS-Prepost, as discussed in the next chapter.

CHAPTER 4

STRUCTURAL RESPONSES OF THE REAR-IMPACT SIMULATIONS

To evaluate the structural responses of the models, the LS-PrePost has been utilized used for post-processing and the D3PLOT of the simulated file is loaded onto the software. Two nodes are selected on the front and the rear bumpers and simulated to identify the maximum intrusion. The nodes are selected with keyword *IDENT and the distance between the nodes is found out using *MEASUR keyword.

4.1 Structural Response of Compact Car (Toyota Yaris)

The structural response of the compact car crash according to the FMVSS 301R is shown in this section. The Toyota Yaris before and after the crash is shown in Figures 4.1 and 4.2.

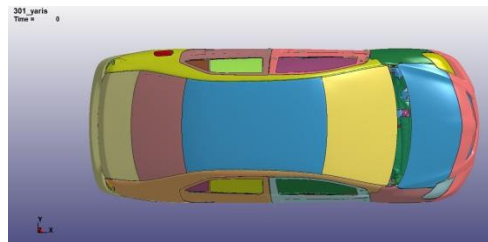


Figure 4.1 Toyota Yaris Before the Crash

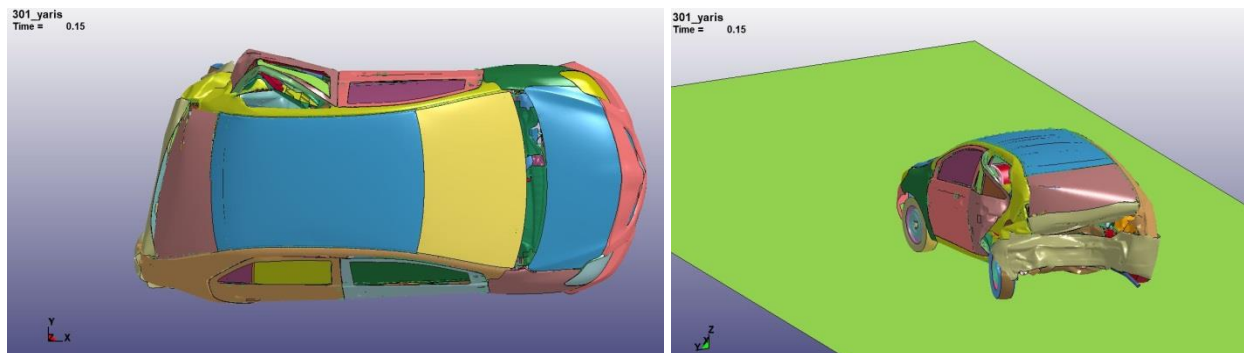


Figure 4.2 Toyota Yaris After the Crash

Figures 4.3 and 4.4 show the overall length of the car before and after the crash. The maximum overall intrusion can be seen at $t=0.115$ s (~11 ms)

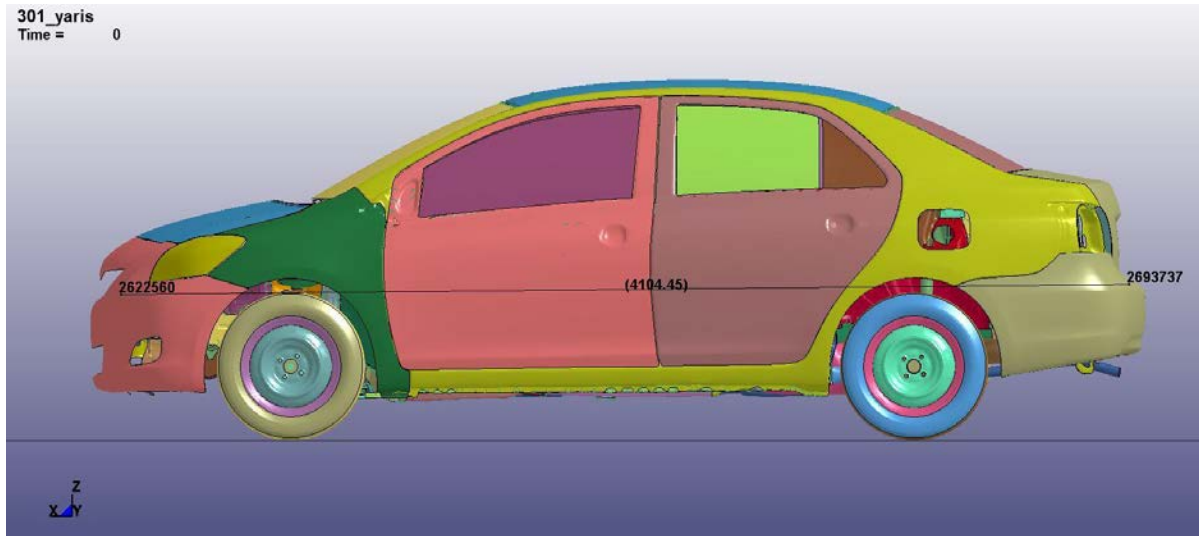


Figure 4.3 Overall Length of Toyota Yaris at $t=0$ ms

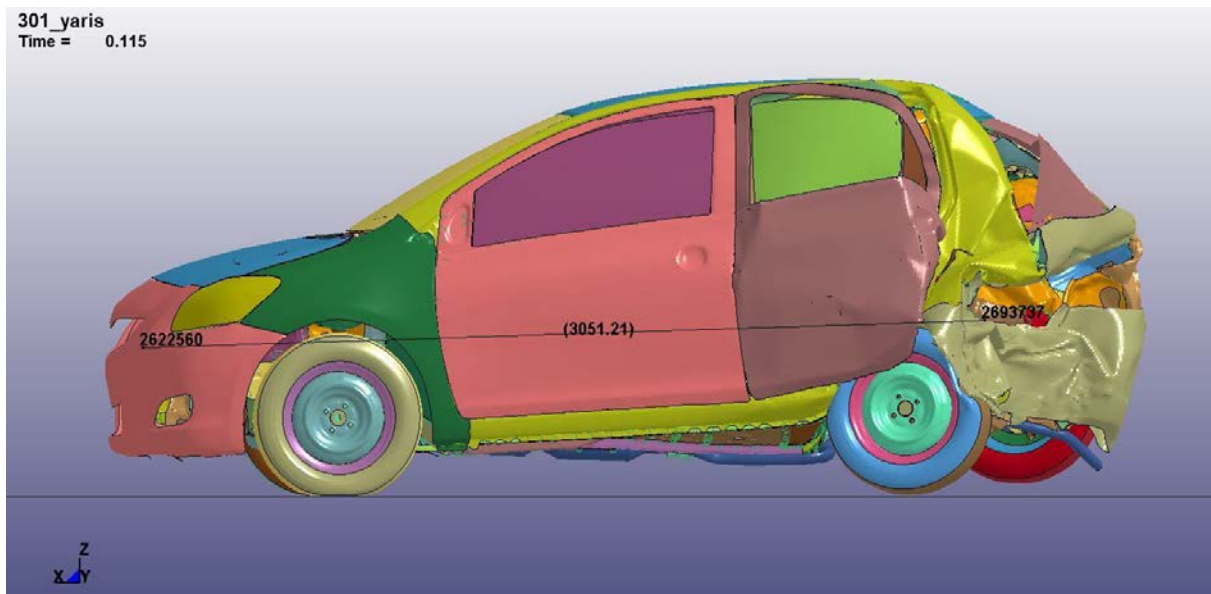


Figure 4.4 Overall Length of Toyota Yaris at $t=11$ ms

Intrusion Length = Change in length = Initial Length – Final Length

$$= 4104 \text{ mm} - 3051 \text{ mm} = \mathbf{1053 \text{ mm}}$$

Similarly, the maximum cabin intrusion, as seen in Figures 4.5 and 4.6 can be measured using the *BLANK keyword to hide the car's roof and using the *IDENT and *MEASUR keywords.



Figure 4.5 Cabin Length of Toyota Yaris at t=0ms



Figure 4.6 Cabin Length of Toyota Yaris at t=15ms

Intrusion Length = Change in length = Initial Length – Final Length

$$= 1643 \text{ mm} - 1479 \text{ mm} = \mathbf{164 \text{ mm}}$$

The longitudinal seat acceleration during the simulation is plotted for the entire duration, as shown in Figure 4.7 and the maximum value is found to be 23g at 12ms.

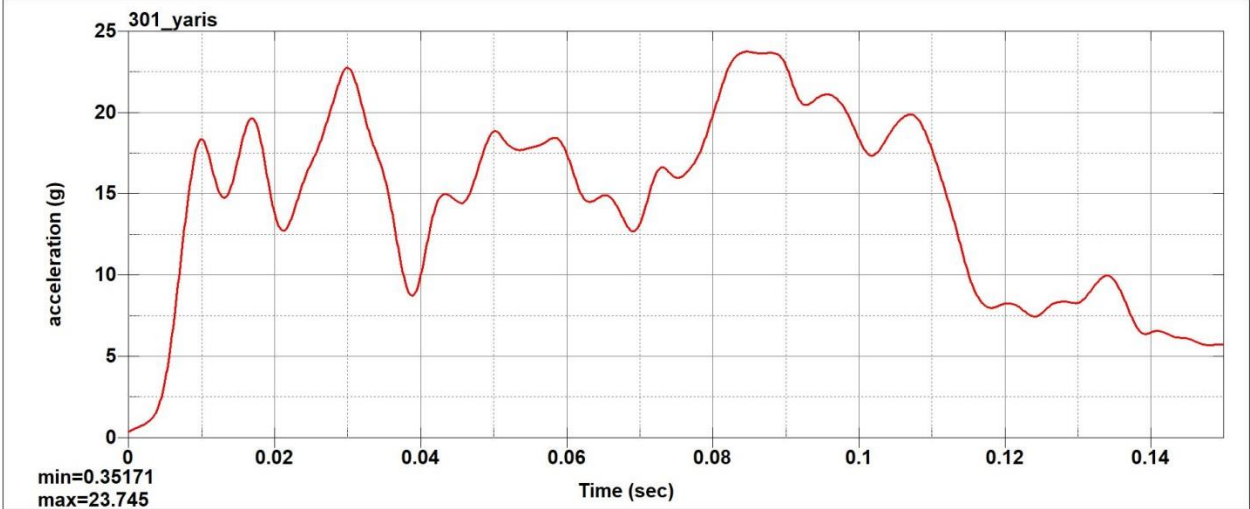


Figure 4.7 Seat Acceleration Plot for Yaris

4.2 Structural Response of Sedan (Toyota Camry)

In this section, the structural responses of a mid-size sedan after the FMVSS 301R crash test simulation are studied. Toyota Camry before and after the crash is shown in Figures 4.8 and 4.9.

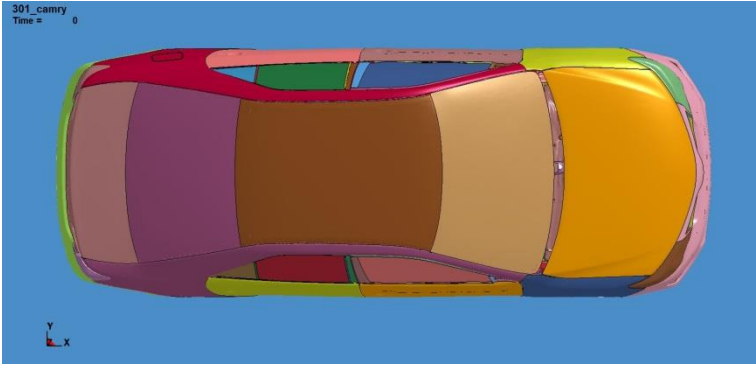


Figure 4.8 Toyota Camry Before the Crash

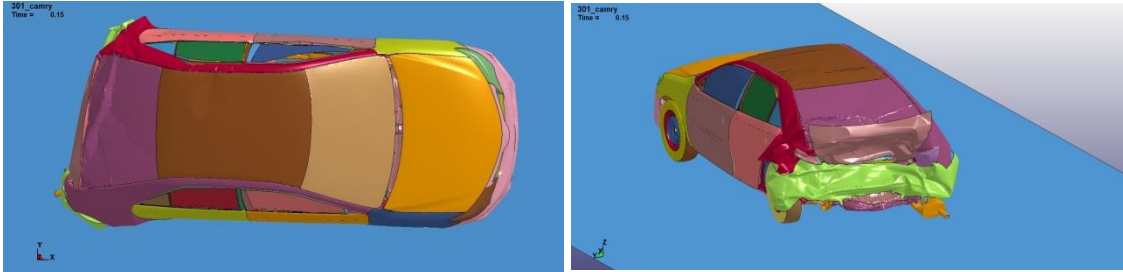


Figure 4.9 Toyota Camry After the Crash

The overall length of the car before and after the crash can be seen in Figures 4.10 and 4.11. The maximum overall intrusion can be seen at $t=0.09$ s (9 ms)

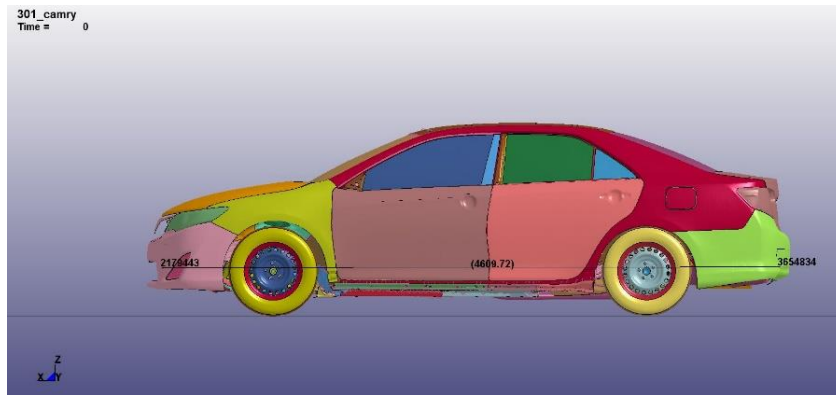


Figure 4.10 Overall Length of Toyota Camry at $t=0$ ms

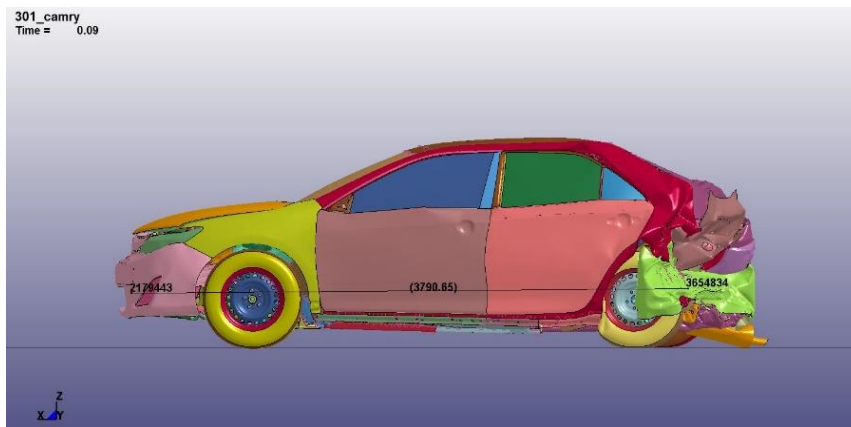


Figure 4.11 Overall Length of Toyota Camry at $t=9$ ms

$$\text{Intrusion Length} = \text{Change in length} = \text{Initial Length} - \text{Final Length}$$

$$= 4609 \text{ mm} - 3790 \text{ mm} = \mathbf{819 \text{ mm}}$$

Similarly, the maximum cabin intrusion, as seen in Figures 4.12 and 4.13 can be measured using the *BLANK keyword to hide the car's roof and using the *IDENT and *MEASUR keywords.

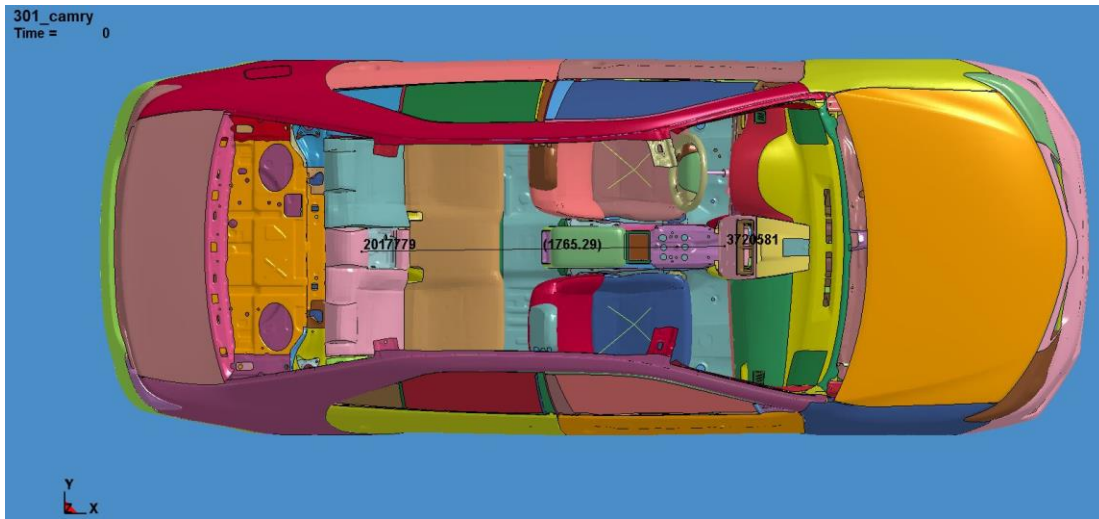


Figure 4.12 Cabin Length of Toyota Camry at t=0ms



Figure 4.13 Cabin Length of Toyota Camry at t=9ms

$$\text{Intrusion Length} = \text{Change in length} = \text{Initial Length} - \text{Final Length}$$

$$= 1765 \text{ mm} - 1670 \text{ mm} = \mathbf{95 \text{ mm}}$$

The seat acceleration during the simulation is plotted for the entire duration, as shown in Figure 4.14 and the maximum value is found to be 22g at 8ms.

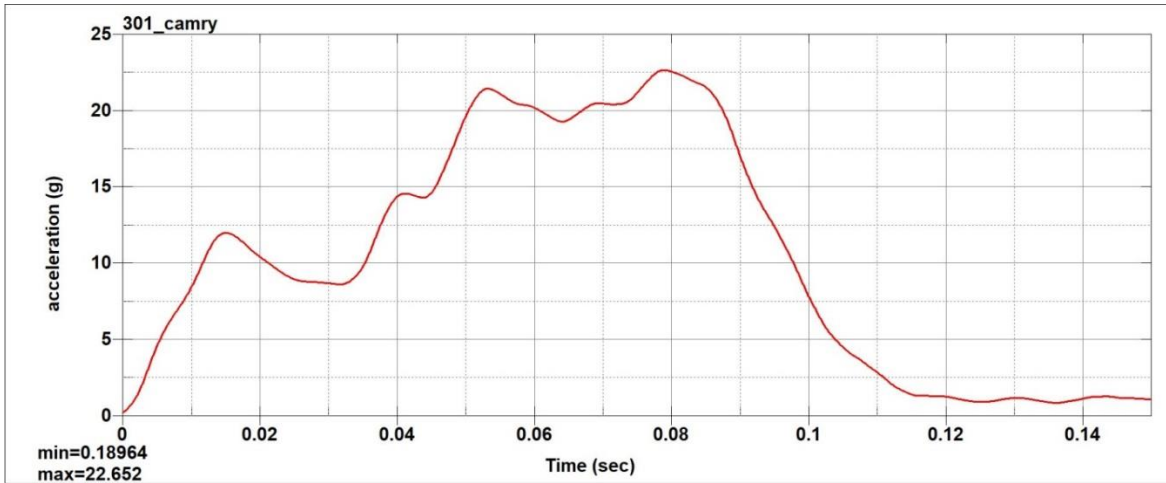


Figure 4.14 Seat Acceleration Plot for Camry

4.3 Structural Response of SUV (Ford Explorer)

The structural response of the SUV after the crash according to the FMVSS 301R is shown in this section. Ford Explorer before and after the crash is shown in Figures 4.15 and 4.16.

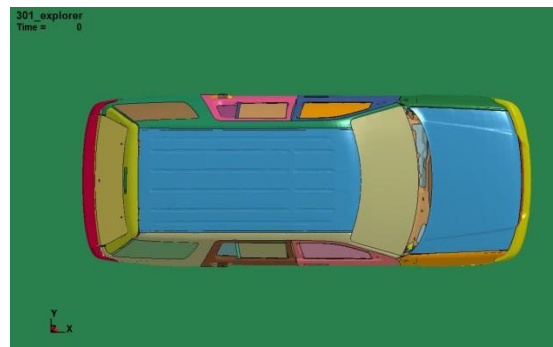


Figure 4.15 Ford Explorer Before the crash

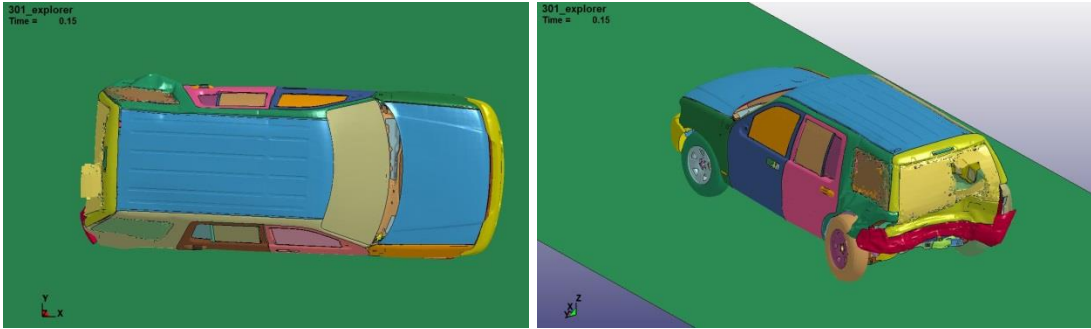


Figure 4.16 Ford Explorer After the crash

Figures 4.17 and 4.18 show the overall length of the car before and after the crash. The maximum overall intrusion can be seen at $t=0.09$ s (9 ms)

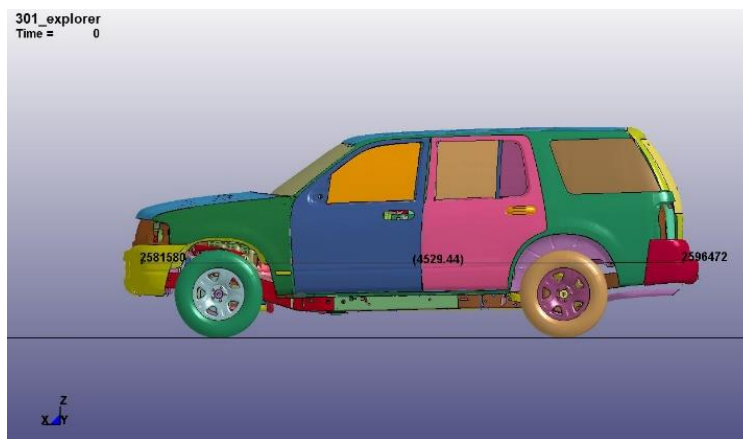


Figure 4.17 Overall Length of Explorer to $t=0$ ms



Figure 4.18 Overall Length of Explorer at $t=9$ ms

Intrusion Length = Change in length = Initial Length – Final Length

$$= 4529 \text{ mm} - 3931 \text{ mm} = \mathbf{598 \text{ mm}}$$

Similarly, the maximum cabin intrusion, as seen in Figures 4.19 and 4.20 can be measured using the *BLANK keyword to hide the car's roof and using the *IDENT and *MEASUR keywords.



Figure 4.19 Cabin Length of Explorer at t=0ms

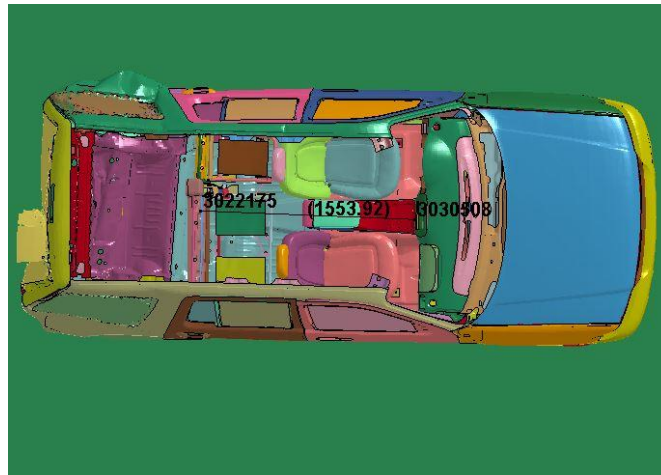


Figure 4.20 Cabin Length of Explorer at t=11ms

Intrusion Length = Change in length = Initial Length – Final Length

$$= 1648 \text{ mm} - 1554 \text{ mm} = \mathbf{94 \text{ mm}}$$

The seat acceleration during the simulation is plotted for the entire duration, as shown in Figure 4.21 and the maximum value is found to be 17g at 8ms.

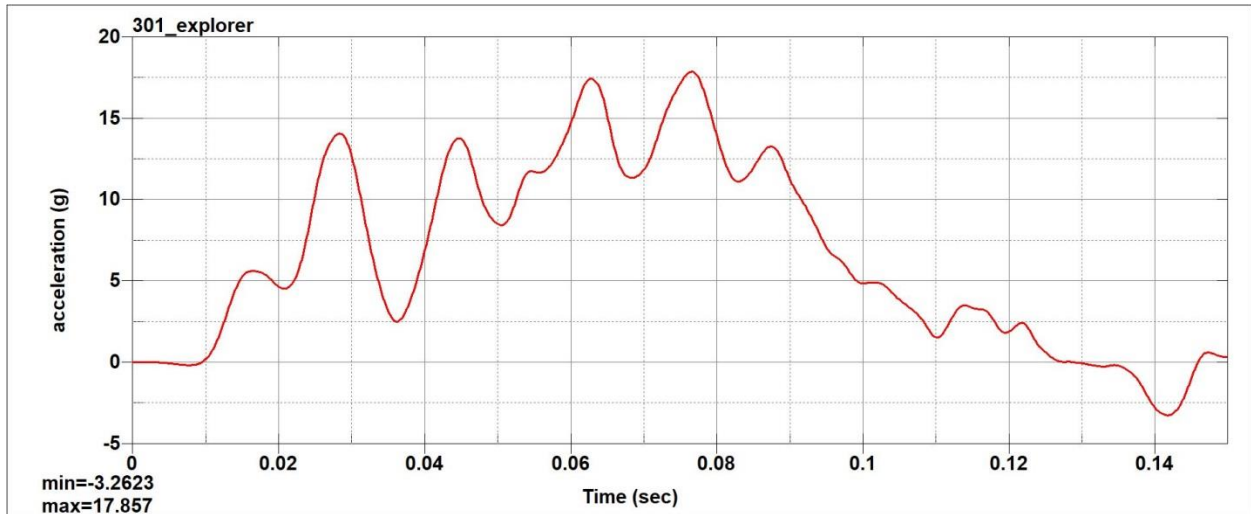


Figure 4.21 Seat Acceleration Plot for Explorer

4.4 Summary of Structural Responses

The structural responses of all the three cars can be seen in Table 4.1. One can observe that the exterior intrusion of the compact car is almost double to that of the SUV. Also, the interior intrusions of sedan and SUV are almost the same. Finally, the seat accelerations of compact car and sedan are relatively close.

Table 4.1 Structural Responses for FMVSS 301R

	Exterior Intrusion (mm)	Interior Intrusion (mm)	Longitudinal Seat Acceleration (g)
Compact Car (Yaris)	1053	164	23.7
Midsize Sedan (camry)	819	95	22.6
SUV (EXplorer)	598	94	17.8

CHAPTER 5

OCCUPANT RESPONSES OF REAR IMPACT SIMULATIONS

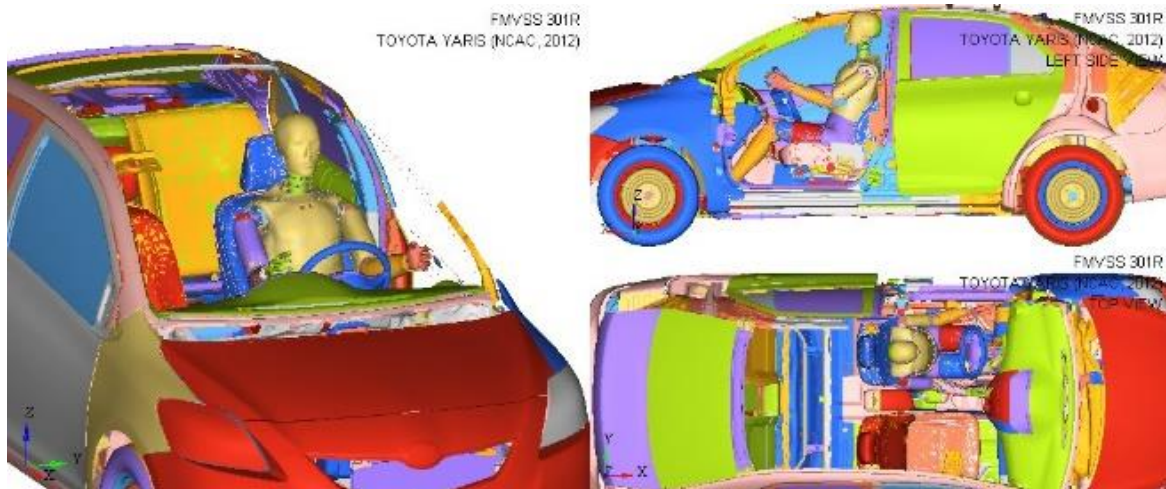
The occupant responses for the rear impact simulations are obtained by reconstructing the test with an occupant (Hybrid III 50th percentile dummy) in the driver seat. The responses can be seen by importing the D3PLOT to Hyperview and using the command *MASK to hide the unnecessary car parts. The joint forces can be found out by loading the 'binout' files in the *BINOUT keyword window. The collected results include:

- Axial force on the neck (F_Z),
- Shear force on the neck (F_X),
- Bending Moment of the neck (M_Y),
- N_{ij} (specifically N_{TE} , for the rear-impact)

All the values are filtered at SAE J211/1rev. Mar 95 Channel Frequency class 600 (SAE, 1995).

5.1 Occupant Responses in Compact Car (Toyota Yaris)

The occupant responses in Toyota Yaris are shown in Figure 5.1. The screenshots of the simulation are taken for every 5ms to observe the responses of the occupant inside the car. The simulations not only show the structural damage, but also the occupant in the car being pushed against the seat as the loads act on the neck, causing significant injury. The simulation is run for about 15 ms and the responses are recorded.

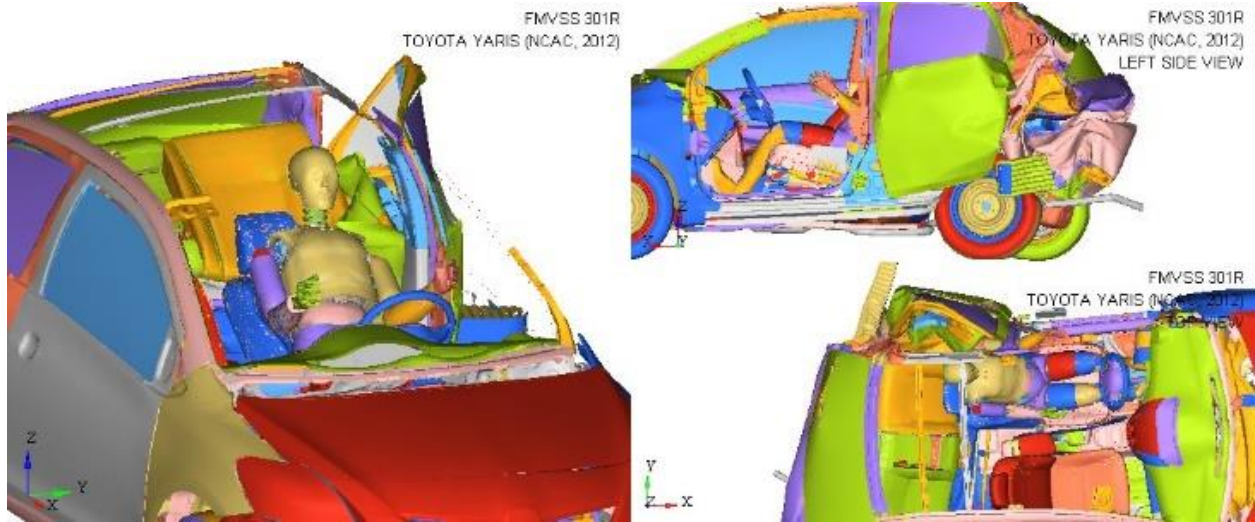


T=0ms

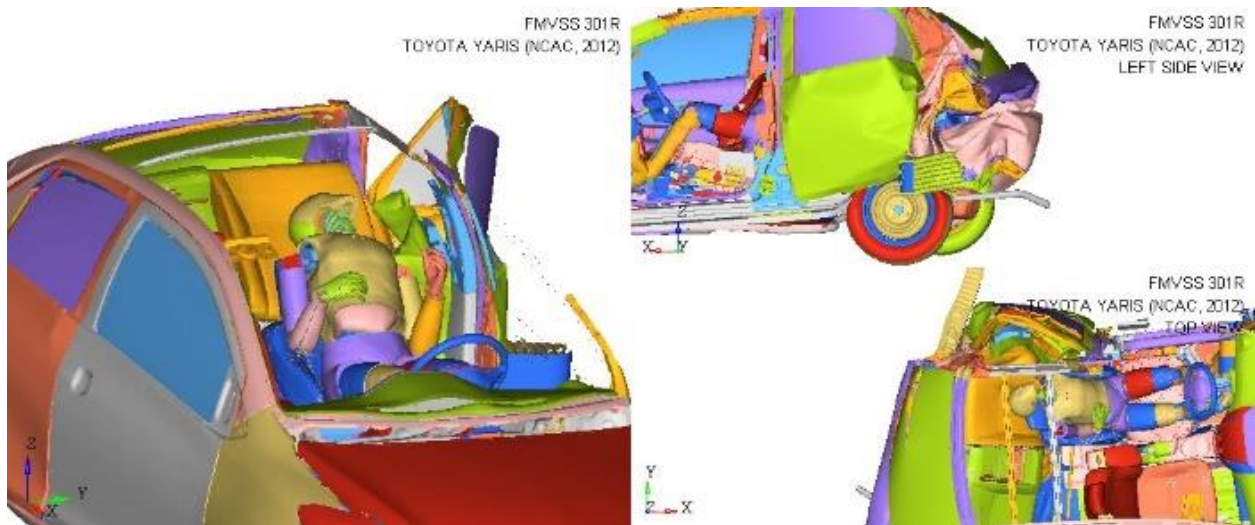


T=5ms

Figure 5.1 Occupant Responses in Toyota Yaris



T=10ms

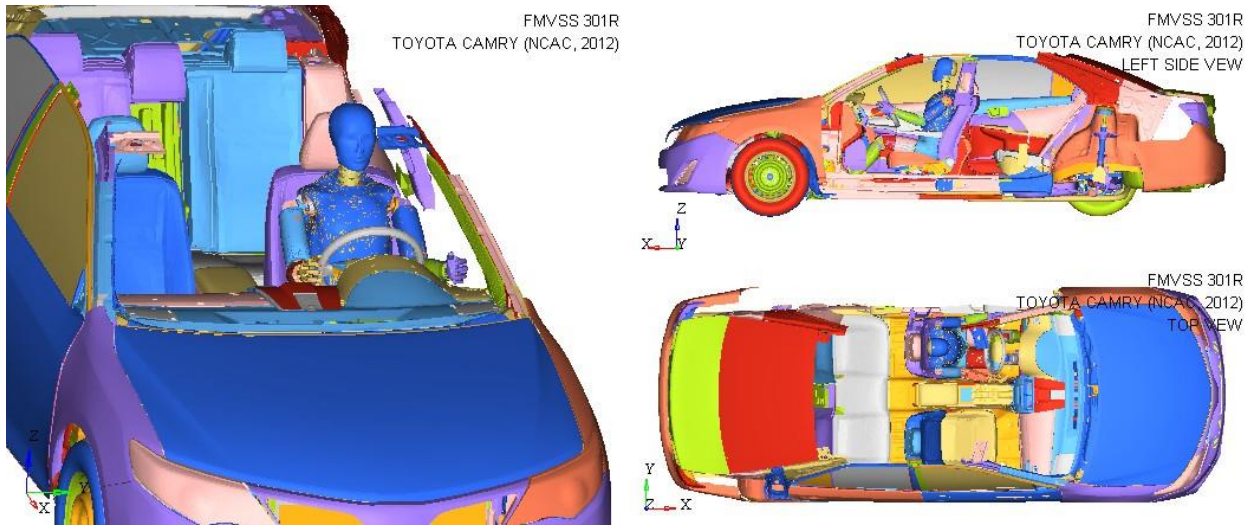


T=15ms

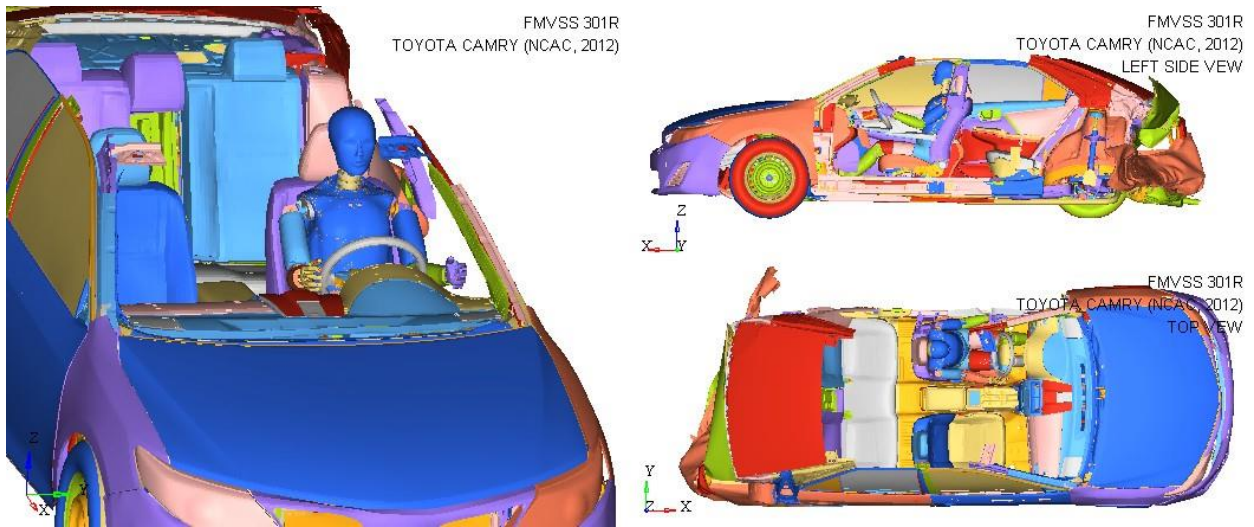
Figure 5.1 Occupant Responses in Toyota Yaris (continued)

5.2 Occupant Responses in Sedan (Toyota Camry)

The occupant responses in Toyota Camry are shown in Figure 5.2. The occupant experiences a significant rear-ward motion as the impact occurs causing injury to the neck. The simulation is run for about 15 ms and the responses after the crash are recorded.

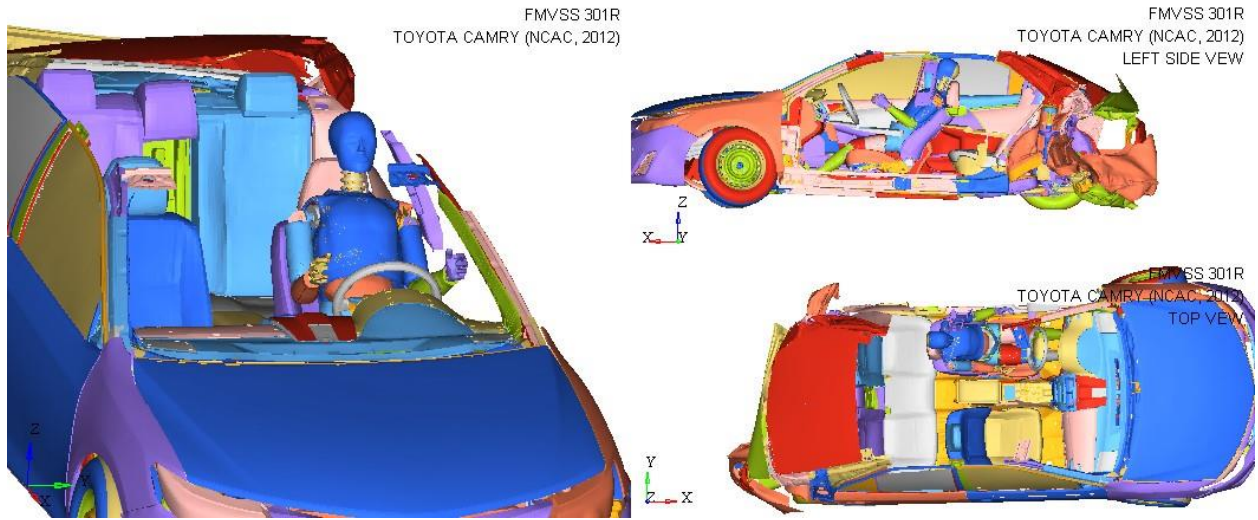


T=0ms

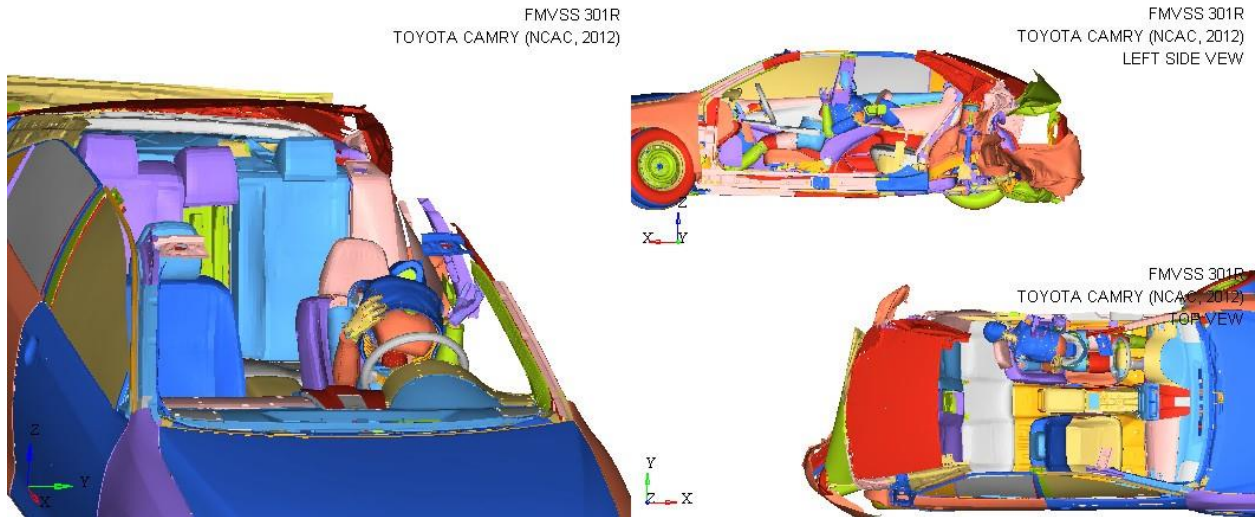


T=5ms

Figure 5.2 Occupant Responses in Toyota Camry



T=10ms

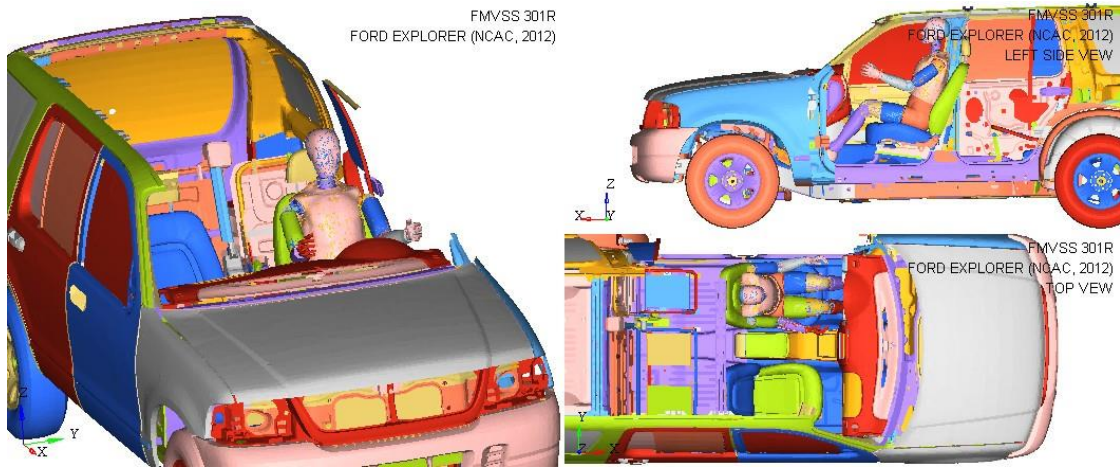


T=15ms

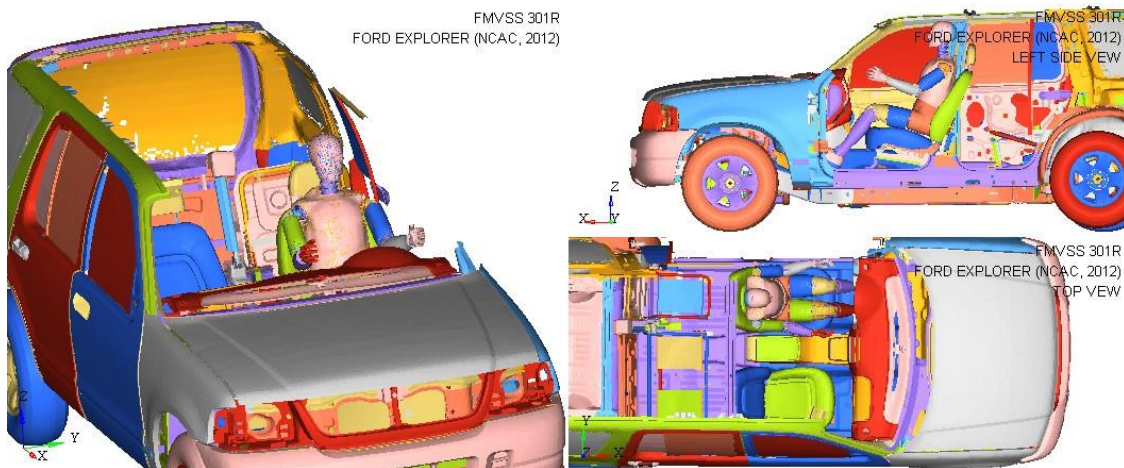
Figure 5.2 Occupant Responses in Toyota Camry (continued)

5.3 Occupant Responses in SUV (Ford Explorer)

The occupant responses in Ford Explorer are shown in Figure 5.3. One can clearly see the difference in the occupant response compared to the other two categories of cars. The simulation is run for about 15 ms and the responses after the crash are recorded.



T=0ms



T=5ms

Figure 5.3 Occupant Responses in Ford Explorer



T=10ms



T=15ms

Figure 5.3 Occupant Responses in Ford Explorer (continued)

5.4 Summary of Occupant Injury Responses

The Neck axial tension load, Neck extension moment, Neck longitudinal shear force and N_{ij} are tabulated in Table 5.1. Looking at the injuries of the occupant, all of the values seem to be below critical injury values, except for the longitudinal shear force in the neck in the compact

car. The neck loads and moments in the compact car are much higher than the SUV and the sedan. The SUV provides much better protection to the occupant in rear-impact than the other two car categories. These values are now used to obtain scatter plots with the structural damage values as input and injury values as output. Then, the best fit lines are formed as detailed in the next chapter.

Table 5.1 Occupant Injuries

Threshold →	Neck Axial Tension Load (N) 4170	Neck Extension Moment (N-m) 57	N_{TE} 1.0	Neck Longitudinal Shear Force (N) 3100
Compact	2128	12.9	0.40	3307
Sedan	1843	3.1	0.29	2266
SUV	710	1.1	0.11	359

CHAPTER 6

LINEAR REGRESSION OF STRUCTURAL AND OCCUPANT RESPONSES FOR PREDICTION OF INJURIES

As mentioned earlier, the data obtained from the simulations of the structural responses and occupant injuries shall be used to predict the occupant injuries. For this, a method called 'Linear Regression' to predict occupant injuries.

Linear Regression is generally used in two ways- Prediction and Response Variation. Since the goal here is to predict the potential injuries, a predictive model is fit to an observed dataset of values after the response. Simply put, the prediction is done based on a line called the 'best-fit line', which is a straight line which best represents the data in the scatter plot. This line may or may not pass through all the points but tries to best predict the possible outcome of a given value based on the trend of the outcomes.

6.1 Linear Regression of Simulation Results

In this research, scatter plots are taken for each pair of inputs and outputs, the input values being the exterior intrusion, interior intrusion, and seat acceleration. The desired outputs are the neck tension, moment, shear and N_{ij} . Thus, there would be a total of 12 plots, three for each of the outputs. These plots are then used to get the best fit line where the equation of the line will be used for calculation. The plots for each of the loads and moments are shown starting from the next page.

6.1.1 Neck Axial Tension Load

The tension load on the neck causes the axial elongation of the neck. The plots for the same are shown in Figures 6.1, 6.2 and 6.3. The exterior intrusion and seat acceleration show a better correlation to the neck tension load than the interior intrusion.

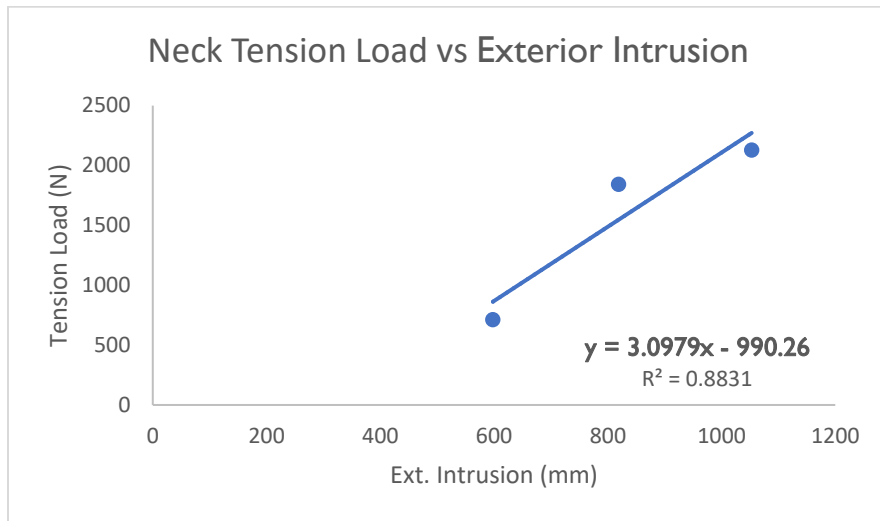


Figure 6.1 Neck Tension Load vs Exterior Intrusion

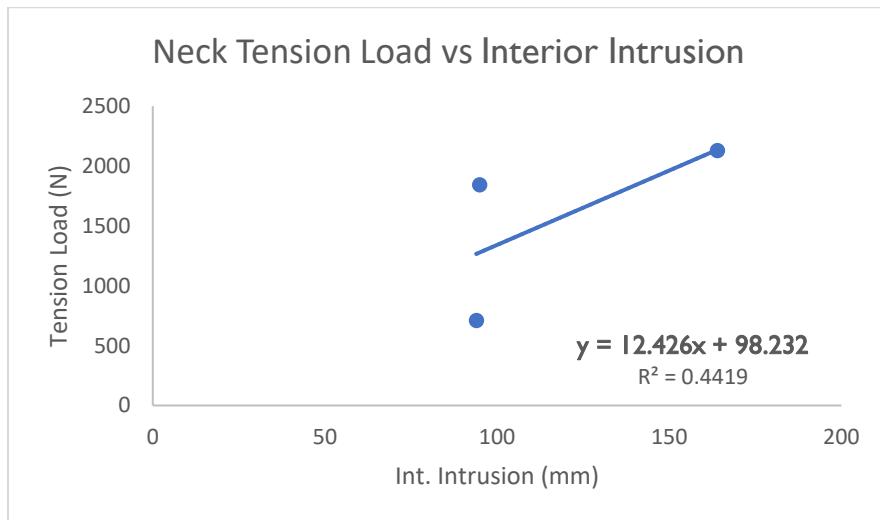


Figure 6.2 Neck Tension Load vs Interior Intrusion

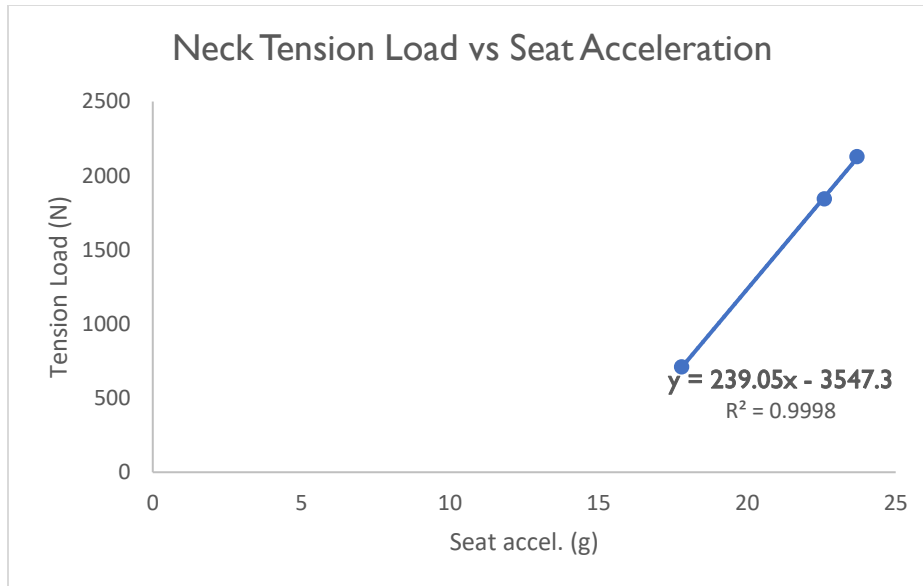


Figure 6.3 Neck Tension Load vs Seat Acceleration

Since the interior intrusion has the least correlation, only the exterior intrusion and the seat acceleration are used to predict neck axial tension load.

6.1.2 Neck Extension Moment

The scatter plots for the neck extension moment is shown in Figures 6.4, 6.5 and 6.6. The interior intrusion shows much little correlation as compared to the exterior intrusion and seat acceleration to the neck bending moment. Therefore, for precise prediction, only the exterior intrusion and the seat accelerations are used to calculate the injuries to the occupant.

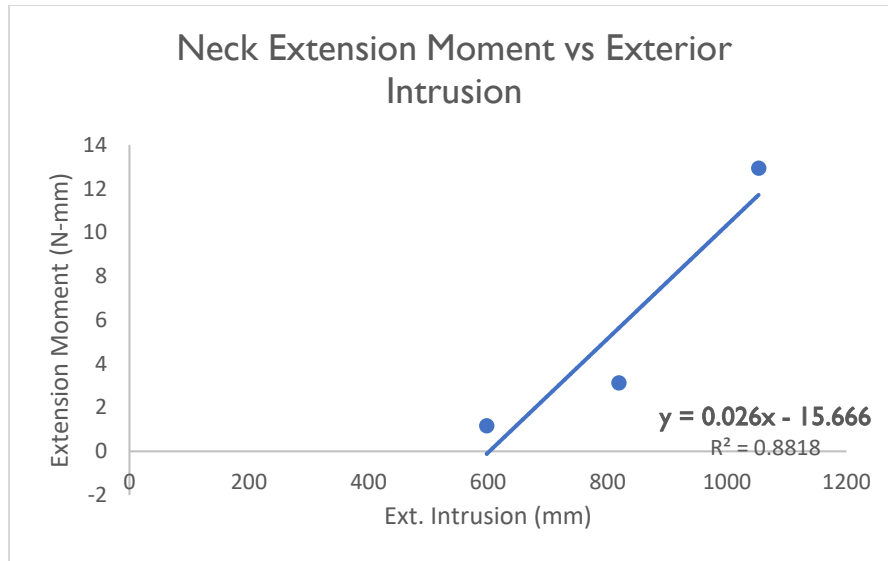


Figure 6.4 Neck Extension Moment vs Exterior Intrusion

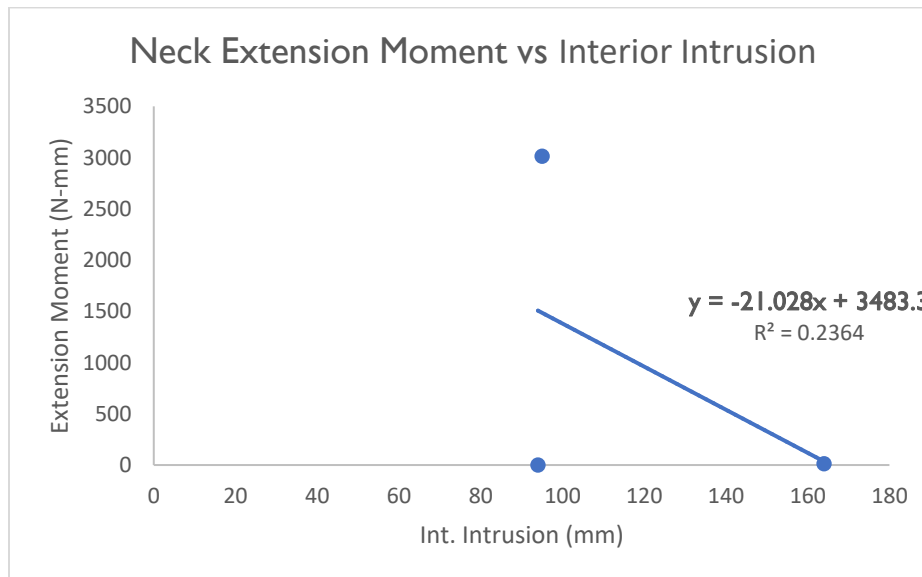


Figure 6.5 Neck Extension Moment vs Interior Intrusion

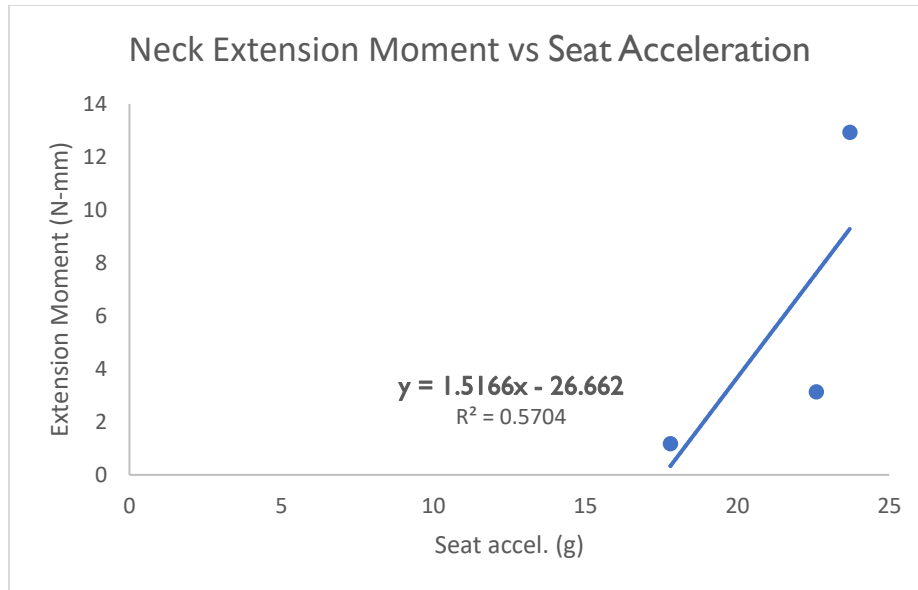


Figure 6.6 Neck Extension Moment vs Seat Acceleration

6.1.3 Neck Longitudinal Shear Force

Even though the shear force on the neck is not considered for the combined loading mechanism, it causes significant injury to the neck. The scatter plots for the neck longitudinal shear force are shown in Figures 6.7, 6.8 and 6.9. The figures show a significant correlation of exterior intrusion and seat accelerations with the shear force on the neck. Although interior intrusion correlates better to the shear force than axial load or bending moment, it is still not considered for injury prediction in this case.

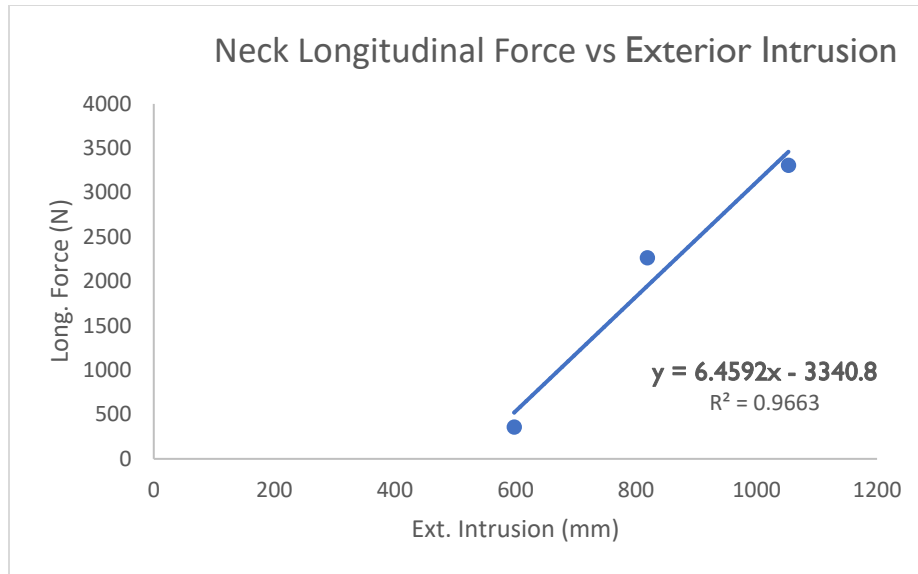


Figure 6.7 Neck Longitudinal Force vs Exterior Intrusion

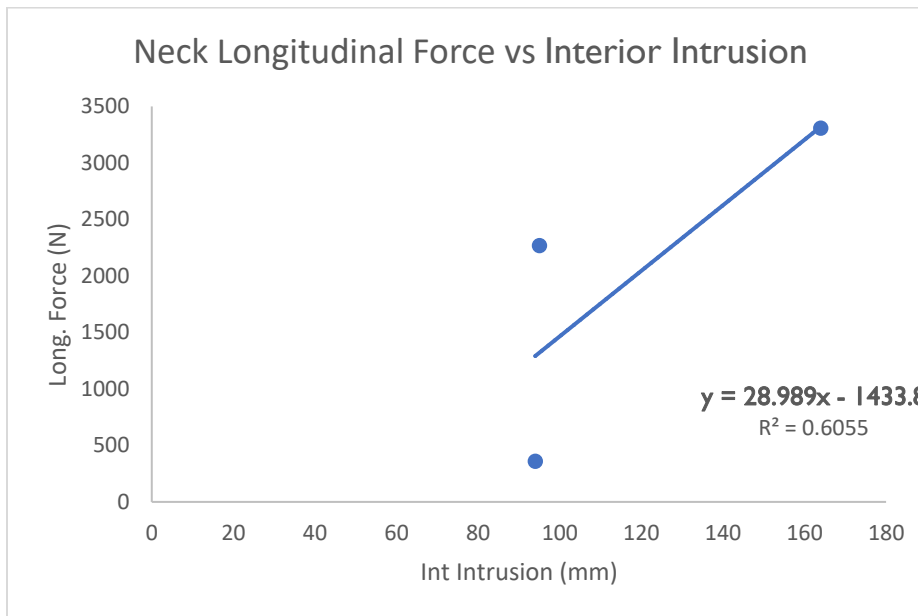


Figure 6.8 Neck Longitudinal Force vs Interior Intrusion

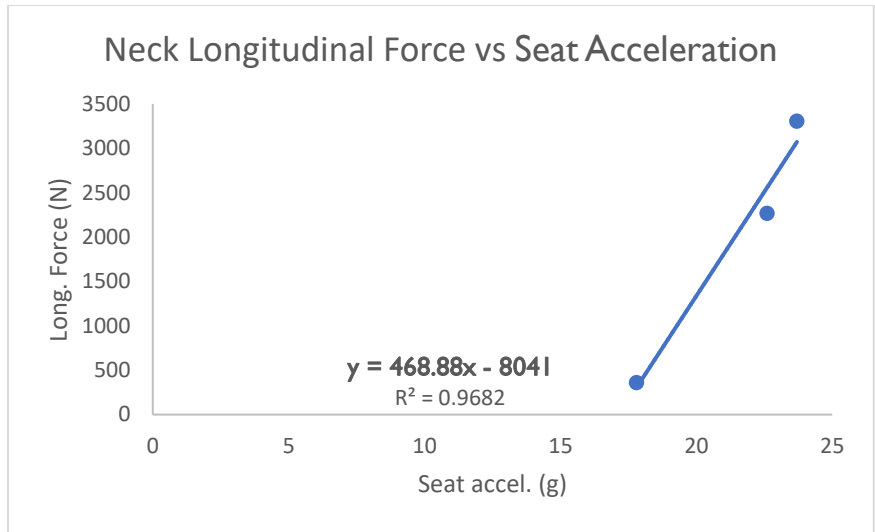


Figure 6.9 Neck Longitudinal Force vs Seat Acceleration

6.1.4 Combined Loading (N_{TE})

The combined loading is calculated based on the neck loads and moments and their critical intercept values as discussed earlier in the neck injury mechanisms (Injury Mechanisms). The scatter plots for N_{TE} are shown in Figures 6.10, 6.11 and 6.12. The regression figures for the N_{ij} also show similar correlations like the neck axial tension load and extension moment and therefore, only these two parameters were used to predict the injuries.

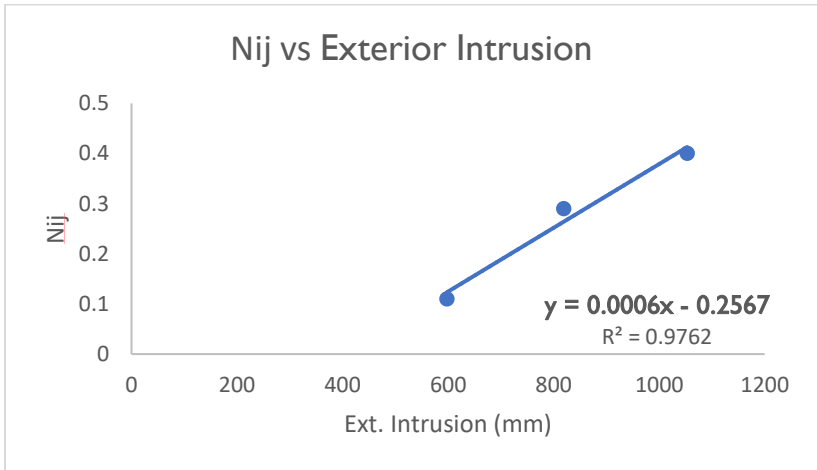


Figure 6.10 Nij vs Exterior Intrusion

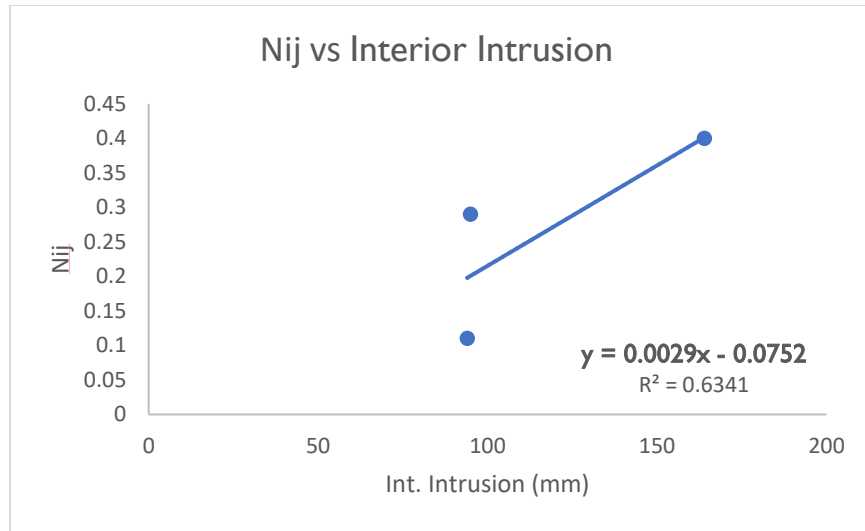


Figure 6.11 Nij vs Interior Intrusion

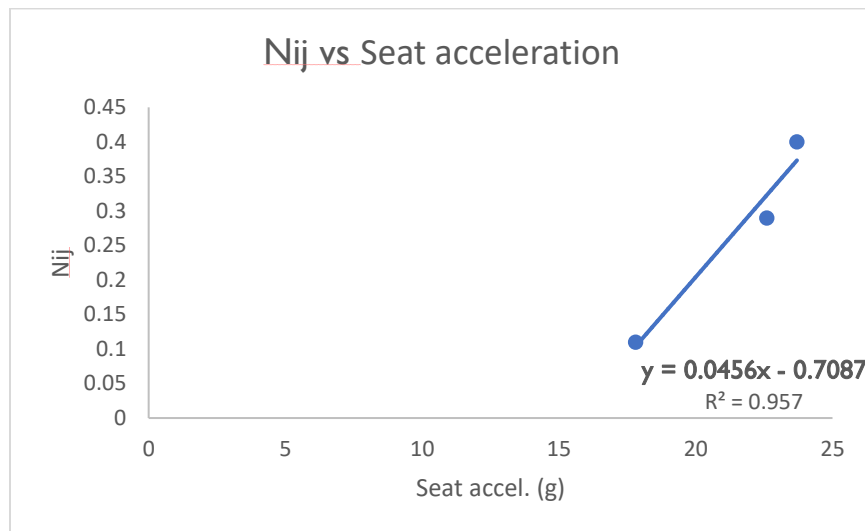


Figure 6.12 Nij vs Seat Acceleration

6.1.5 Prediction using Linear Regression

There are quite a few observations made from the linear regression of the simulation results. Firstly, there is a linear relationship between the structural damage and the injuries in a

rear-impact. Seat accelerations seem to correlate to the injuries the most while the Interior Intrusion has the least correlation. Therefore, only the exterior intrusion and seat acceleration were used for injury prediction.

The linear regression model is checked for accuracy by using the obtained equations and calculating the injuries of the earlier simulated cars. The results are shown in Table 6.1. While the bending moment could not be predicted accurately, the neck axial tension load, shear force and N_{TE} were predicted with less than 10% maximum error. One can observe that the prediction error in bending moment gradually increases from compact car to SUV, the errors for the remaining injury parameters are under 10%. Therefore, this method can be utilized to predict the injuries without using the dummy and the cars which don't have seats available.

Table 6.1 Predicted Injuries

Threshold	Neck Axial Tension load (N) 4170			Neck Extension moment (N-m) 57			N_{TE} 1.0			Neck Longitudinal Shear Force (N) 3100		
	Predicted	Actual	Error %	Predicted	Actual	Error %	Predicted	Actual	Error %	Predicted	Actual	Error %
Compact	2194	2128	3.1	10.45	12.9	18.0	0.38	0.40	5.0	3265	3307	1.2
Sedan	1700	1843	7.7	4.1	3.1	32.2	0.27	0.29	10.0	2249	2266	0.72
SUV	784	710	5.3	0.71	1.1	35.4	0.10	0.11	9.0	396	359	10.3

6.2 Rear-Impact Test Simulations of Additional Cars for Injury Prediction

The rear-impact test simulations are conducted on three additional cars to extract exterior and interior intrusions, and seat accelerations, wherever applicable. The FE models of the cars are discussed before the modeling the simulations.

6.2.1 Dodge Neon

The compact car used for the verification of injury predictions is a Dodge Neon. The FE model was reverse engineered at the George Washington University. This was done by the NCAC in 2006 (National Crash Analysis Center, 2006). The FE isometric model and detailed interior models are shown in Figures 6.13 and 6.14.



Figure 6.13 FE Model of a 1996 Dodge Neon (*National Crash Analysis Center, 2006*)



Figure 6.14 Dodge Neon FE Model Interior View (*National Crash Analysis Center, 2006*)

The summary of the FE Model is shown in Table 6.2.

Table 6.2 Dodge Neon FE Model Summary (*National Crash Analysis Center, 2006*)

Model	1996 Dodge Neon
Number of Parts	336
Number of Nodes	283,859
Number of Shells	267,786
Number of Beams	122
Number of Solids	2852
Number of Elements	270,768

6.2.2 Ford Taurus

The sedan used for the verification of injury predictions is a Ford Taurus. The FE model was reverse engineered at the George Washington University. It was done by the NCAC in 2012 (Marzougui, 2012). The FE isometric model is shown in Figure 6.15

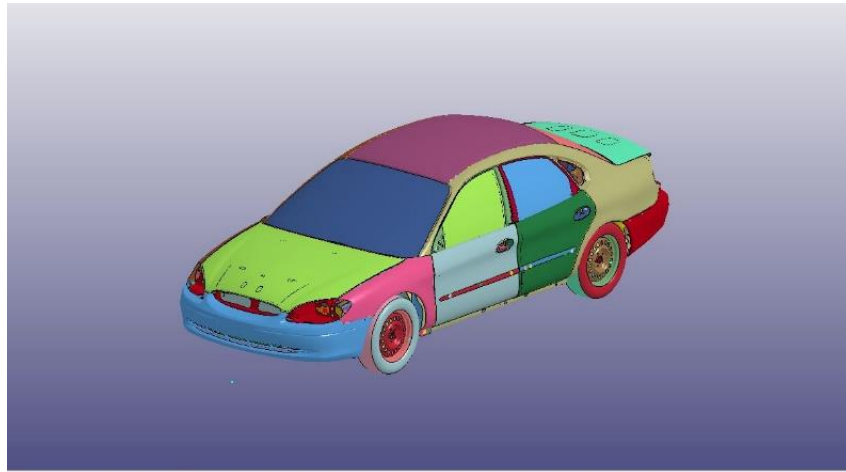


Figure 6.15 FE Model of 2001 Ford Taurus

The FE model summary of the car is shown in Table 6.3.

Table 6.3 Ford Taurus FE Model Summary (Marzougui, 2012)

Model	2001 Ford Taurus
Number of Parts	802
Number of Nodes	921,793
Number of Shells	838,880
Number of Beams	10
Number of Solids	134,449
Number of Elements	973,351

6.2.3 Dodge Caravan

Dodge Caravan is the van class car used for the research. The Finite element model was reverse engineered at the George Washington University. It was done by the NCAC in 2007 (National Crash Analysis Center, 2007). The FE isometric model is shown in Figure 6.16.

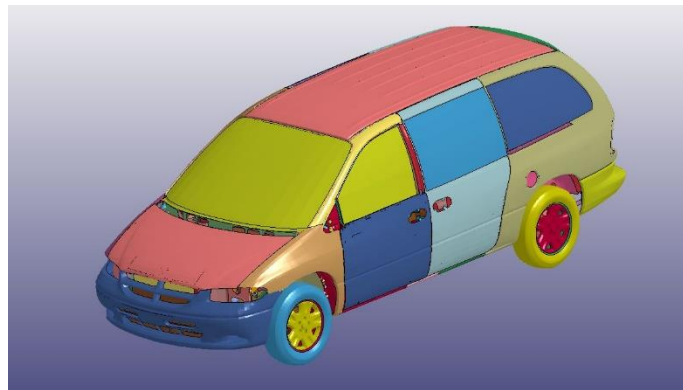


Figure 6.16 FE Model of 1997 Dodge Caravan

The FE model summary of the car is shown in Table 6.4.

Table 6.4 Dodge Caravan FE Model Summary (*National Crash Analysis Center, 2007*)

Model	1997 Dodge Caravan
Number of Parts	510
Number of Nodes	344,724
Number of Shells	327,163
Number of Beams	35
Number of Solids	6253
Number of Elements	333,455

6.2.4 Structural Responses of Additional Cars after Rear-end Crash Simulation

The FMVSS 301R test simulation modeling of each of the cars mentioned earlier is shown in Figures 6.17, 6.18 and 6.19

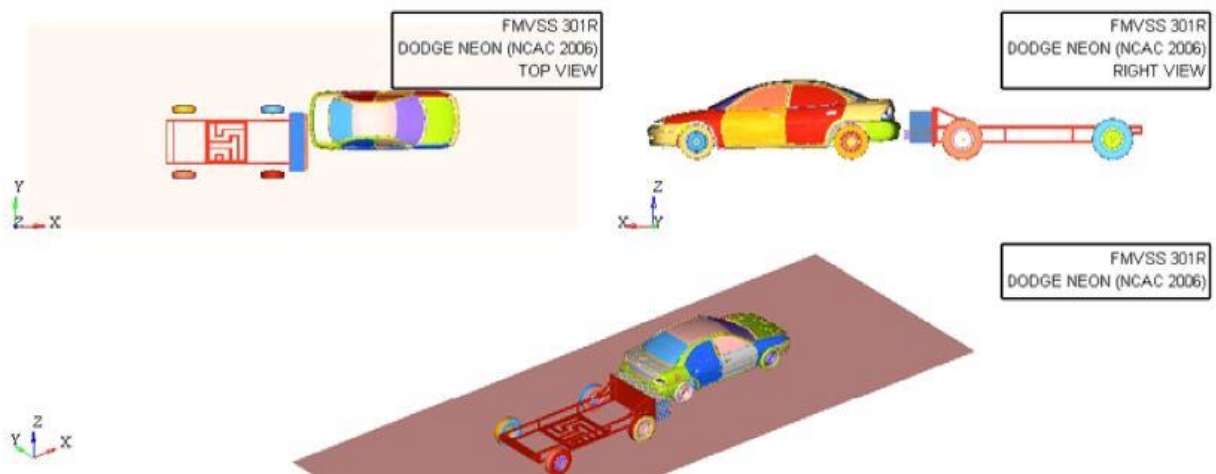


Figure 6.17 Rear-Impact modeling of Dodge Neon

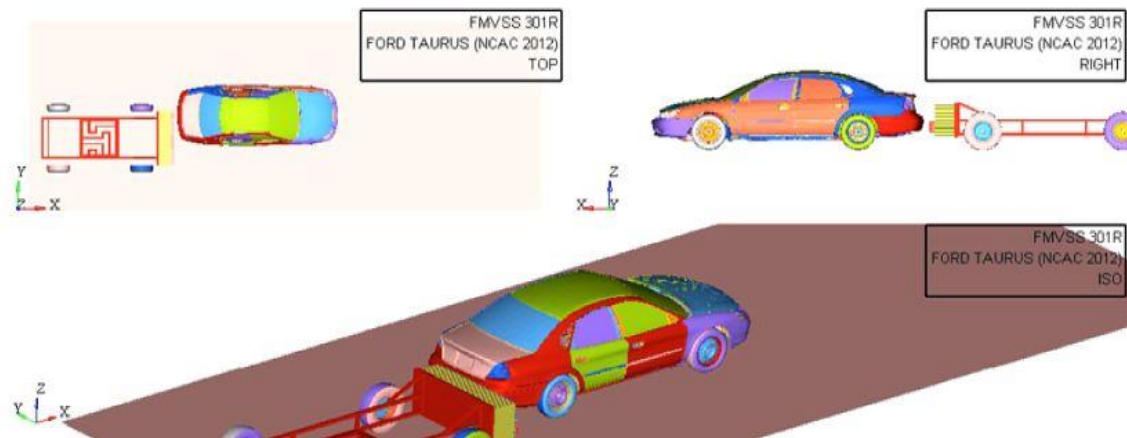


Figure 6.18 Rear-Impact modeling of Ford Taurus

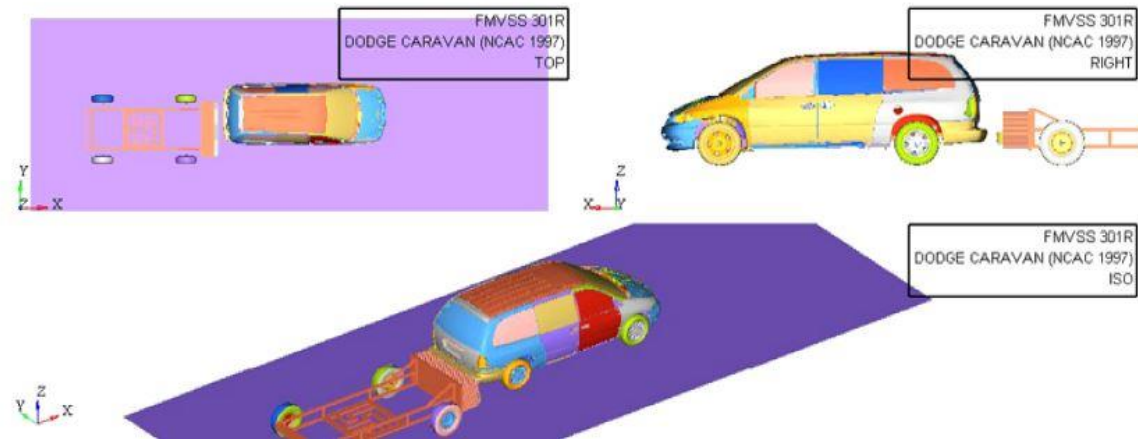


Figure 6.19 Rear-Impact modeling of Dodge Caravan

The structural responses of all the three cars are shown in Figures 6.20, 6.21 and 6.22. These figures show the cars before and after the crash simulation. Two sets of nodes are selected on the front and the rear bumpers as well as in the inside of the cabin and simulated to identify the maximum exterior and interior intrusion respectively. The nodes are selected with keyword *IDENT and the distance between the nodes is found out using *MEASUR keyword.

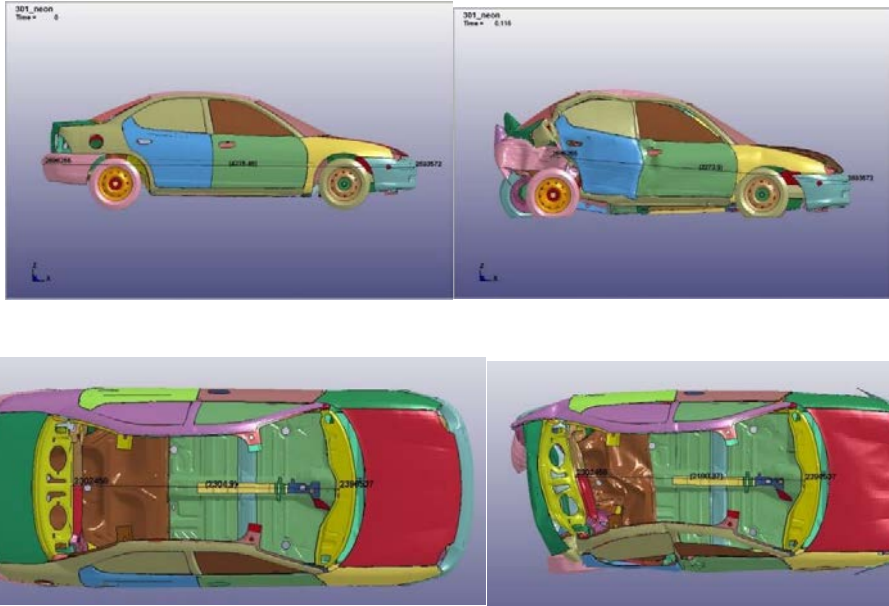


Figure 6.20 Structural Responses of Dodge Neon

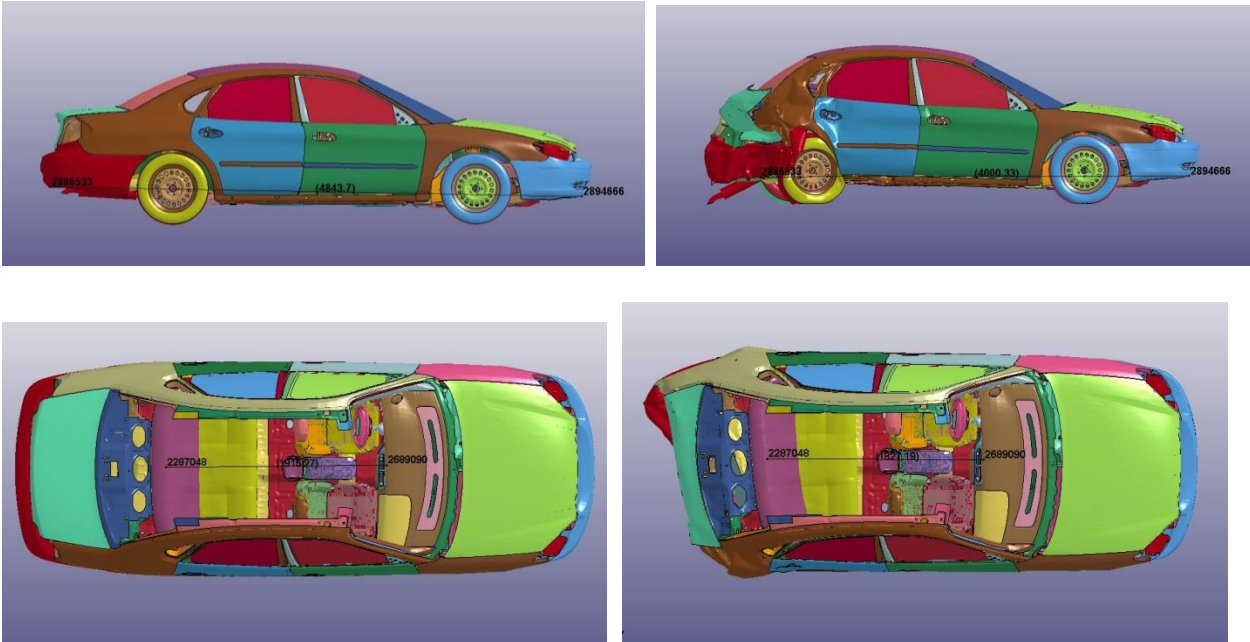


Figure 6.21 Structural Responses of Ford Taurus

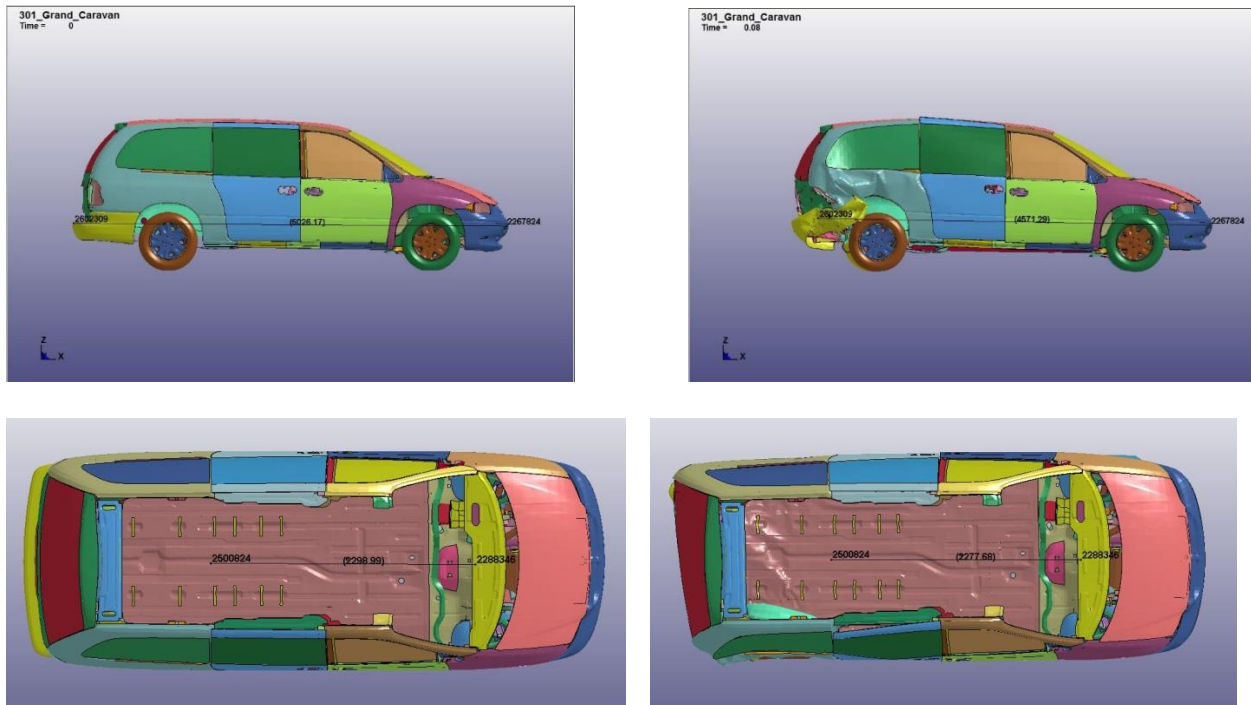


Figure 6.22 Structural Responses of Dodge Caravan

The structural responses of all the three cars are tabulated in Table 6.5.

Table 6.5 Structural Responses of the Additional Cars

	Exterior Intrusion (mm)	Interior Cabin Intrusion (mm)
Dodge Neon	1002	114
Ford Taurus	843	94
Dodge Caravan	445	21

Now, by substituting the values of Exterior and Interior Intrusions (inputs) in the regression line equation to predict the neck injuries (outputs). These results are tabulated in Table 6.6.

Table 6.6 Predicted Occupant Injuries for the Additional Cars

Threshold →	Neck Axial Tension Load (N) 4170	N_{TE} 1.0	Neck Longitudinal Shear Force (N) 3100
Dodge Neon	2113	0.34	3131
Ford Taurus	1621	0.24	2104
Dodge Caravan	388	0.01	466

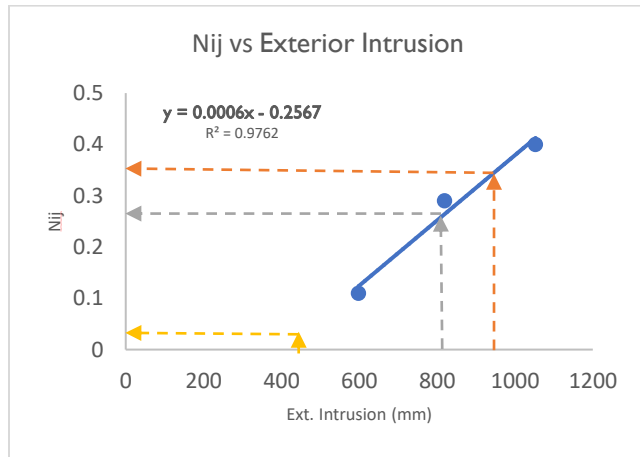
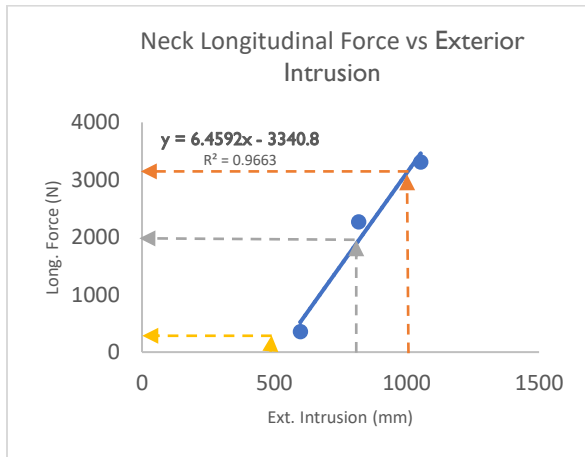
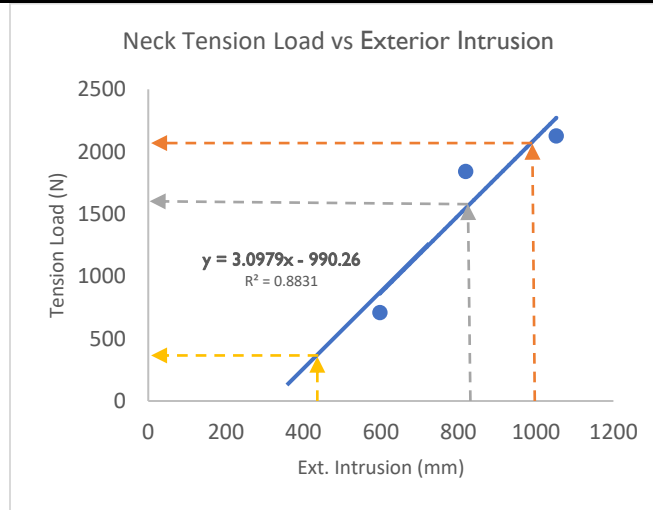


Figure 6.23 Predicted Injuries for Additional Cars

The calculated values of the injuries seem to be following the same trend as the original three cars (Yaris, Camry, and Explorer) have.

CHAPTER 7

CONCLUSIONS AND RECOMMENDATIONS

7.1 Conclusions

The goal of this study was to investigate the correlation between the structural damage as well as the occupant responses in an automobile in a rear-impact under FMVSS 310R test conditions. Rear-end collisions, especially high-speed collisions are not only responsible for high structural damage, but also significant injury to the occupant. This test was particularly chosen because not much study has been done about the occupant injuries when there is a rear-impact. The FMVSS 301R fuel system integrity test was conducted on three different categories of cars with and without a 50th percentile Hybrid III male dummy.

Three cars (Toyota Yaris, Toyota Camry, and Ford Explorer) were used as initial models for the rear-impact test simulations. The exterior and interior intrusions along with the seat accelerations were recorded. Next, the test was performed again with the occupant inside to get the neck injury values (tension load, extension moment and shear force). The N_{ij} values were calculated using the axial tension load and the bending moment. Except for the neck longitudinal shear force in a small car, all the other neck loads were within the threshold limits. Although the loads and moments on the occupant were within the limit, the effects could be long-lasting.

The results were then used for linear regression to produce correlations for the prediction of potential injuries. The observations from the linear regression of the simulations revealed that there is a linear relationship between the structural exterior damage and the injuries associated with the rear-impact. Therefore, this method can be utilized to predict the injuries without using the dummy and or the cars which do not have seats available.

The following specific conclusions can be made from this study.

- Exterior intrusion of the compact car is almost double to that of the SUV and Interior intrusions of sedan and SUV are almost the same.
- There does not seem to be much difference in interior intrusions as opposed to the exterior intrusion values, which have a large variation.
- Seat accelerations of compact car and sedan are relatively close.
- Except for the Neck longitudinal shear force in Toyota Yaris, all the other neck loads and moments are within the threshold limits and are much higher in compact car than in sedan and SUV.
- SUV provides much better protection to the occupant in rear-impact than the other car categories.
- Seat accelerations seem to best correlate to the injuries, while the interior intrusion provided the least precise prediction. Therefore, only the exterior intrusion and seat acceleration were used to predict potential injury to the occupant.
- While the bending moment could not be accurately predicted, the neck axial tension load, neck shear force, and N_{TE} were all predicted for about 10% maximum error.
- Extracting the seat accelerations might have helped in much precise prediction. The interior intrusion is observed to have the least effect in deciding the outcome on the injuries.
- In general, the structural damage in rear-impact for sedan and SUV were 27% and 45% lower to the small car, respectively.
- Similarly, the injury potential to the occupant in a small car in rear-impact is 51% and 135% more than sedan and SUV.

- It is recommended that this fuel tank safety test be utilized by the automobile industry for the evaluation of structural integrity and occupant injuries in rear-end crashes.

7.2 Recommendations

The following future recommendations are identified in extending the current research.

- It is important to develop a regulatory standard for occupants in rear-impacts protection by the NHTSA.
- More injury parameters such as lumbar loads and chest accelerations can be studied and predicted.
- As more data is gathered on the crash scenarios, statistics and DOE can be applied to aid for more precise prediction.
- The research can be repeated with the driver wearing a seatbelt.
- A normalized value in terms of exterior intrusion, interior intrusion, and seat acceleration can be utilized as a metric for evaluation or rating of different cars in rear-impacts.

REFERENCES

REFERENCES

- AAAM. (2018). "Abbreviated Injury Scale (AIS)", The Association for the Advancement of Automotive Medicine. <https://www.aaam.org/abbreviated-injury-scale-ais/>[retrieved December 2018]
- Altair Engineering. (2014). "Hyperworks".<https://altairhyperworks.com/>[retrieved December 2018]
- Hassan A., M. (2005). "Comparision of Structural Damage and Occupant Injuries Corresponding to a Vehicle Collision into a Pole Versus a Flat Barrier".MS Thesis,: Wichita State University, Wichita.
- Atahan, A. (2003). "Design and Simulation of an Energy Absorbing Underride Guard for Heavy Vehicle Rear-End Impacts". *International Journal of Heavy Vehicle Systems*, 10(4).
- Avery, e. a. (2006). "The Development of a New Low-Speed I0mpact Test to Improve Bumper Performance and Compatibility". *International Journal of Crashworthiness*, 11(6), 573-581. <https://trid.trb.org/view/809975>[retrieved December 2018]
- Dassault Systemes. (2018, October 18). *DSS CATIA*. <https://www.3ds.com/products-services/catia/>[retrieved December 2018]
- Derosia, et al., (2003). "Rear Impact Responses of Different Sized Adult Hybrid III Dummies". *Traffic Injury Prevention*, 5(1),50-55.
- Eriksson, L., and Boström, O. (1999). "Assessing the Influence of Crash Pulse, Seat Force Characteristics, and Head Restraint Position on NIC in Rear-End Crashes using a Mathematical BioRID Dummy". *IRCOBI Conference*. Sitges, Spain.
- Federal Motor Vehicle Safety Regulations*. (2018). (National Highway Traffic Safety Administration) Regulations: <https://www.nhtsa.gov/laws-regulations/fmvss>[retrieved December 2018]
- Heinrichs, B. E., Lawrence, J. M., Allin, B. D., Bowler, J. J., Wilkinson, C. C., Ising, K. W., Ptucha, S. J. (2001). Low-Speed Impact Testing of Pickup Truck Bumpers. *SAE transactions*, 110(6), 1077-1099. <https://sae.org/publications/technical-papers/content/2001-01-0893>[retrieved December 2018]
- Herbst, B. R. (2009). "Rear-Impact Test Methodologies: Quasistatic and Dynamic Tests". *Safety Analysis & Forensic Engineering (S.A.F.E)*.
- Jagan, B. (2004). "An Optimised Interior Vehicle Configuration for Low Speed Rear-End Impact in a Mid-Sized Sedan". MS Thesis, Wichita State University, Wichita.

- Jugge, V. (2017). "A Computational Methodology for Evaluation of the Structural Damage a to a Car and its Occupant Response for the New FMVSS 310R Regulation as well as for various Real-World Rear-end Collision Scenarios". MS Thesis, Wichita State University, Wichita:
- Kalaga, S. S. (2018). "Evaluation of Far-Side Occupant Injuries and Interaction with Nearside Pccupant Under FMVSS 214 Side Impact Test Requirements". MS Thesis, Wichita State University, Wichita:
- Kleinburger, et al., (1999). "Effects of Head Restraint Position on Neck Injury in Rear Impact". *Proceedings of the World Congress on Whiplash and Associated Disorders*. Vancouver, Canada.
- Kuppa, S., Saunders, J., & Stammen, J. (2006). Kinematically Based Whiplash Injury Criterion.: NHTSA. East Liberty, Ohio.
- Lankarani, H. M. (2017). Spine Injury Biomechanics. Wichita State University, Wichita.
- Leiss, P. J. (2014). "Vehicle Safety – Expert Introduction to Crashworthiness". (Robson Forensic) <https://www.robsonforensic.com/articles/vehicle-safety-expert-introduction-to-crashworthiness>[retrieved December 2018]
- Livermore Software Technology Corporation (LSTC). (2007, May). *LS-DYNA*. "Keyword User's Manual".
- Livermore Software Technology Corporation. (2011). *LS-DYNA*. <http://www.lstc.com/products/ls-dyna>[retrieved December 2018]
- Livermore Software Technology Corporation. (n.d.). Download LSTC Dummy and Barrier Models for LS-DYNA. (LSTC) from http://www.lstc.com/download/dummy_and_barrier_models[retrieved December 2018]
- Martin, G. Y. (2002). "The Crash Pulse in Rear-End Car Accidents ". Gothenburg, Germany
- Marzougui,D. (2012). "Extended Validation of the Finite Element Model for the 2010 Toyota Yaris". The National Crash Analysis Center. Ashburn, Virginia.
- Marzougui, D. (2012). "Extended Validation of the Finite Element Model for the 2001 Ford Taurus Passenger Sedan". The Natinal Crash Analysis Center. Ashburn, Virginia.
- Marzougui, D. (2012). "Extended Validation of the Finite Element Model for the 2002 Ford Explorer Sport Utility Vehicle". The National Crash Analysis Center. Ashburn, Virginia.
- Mats Y, S., Ola, B., Johan, D., Hans-Arne, H., Yngve, H., Per, L., Anette, S. (2000)."Neck Injuries in Car Collisions — a Review Covering a Possible Injury Mechanism and the Development of a New Rear-Impact Dummy". *Accident Analysis & Prevention*, 167-175.
- Mertz, H., & Patrick, L. (1971). "Strength and response of the human neck". *15th Stapp Car Crash Conf*. Coronado, CA
- Murphy, D. (2009, September 28). "Chiropractic Treatments for Whiplash". *Spine-Health*, 19(17).

- National Center for Collision Safety and Analysis. (2016). "Development & Validation of a Finite Element Model for the 2012 Camry". George Mason University, Fairfax, Virginia.
- National Crash Analysis Center. (2006). "Finite Element Model of Dodge Noen". NHTSA, Ashburn, Virginia.
- National Crash Analysis Center. (2007). "FE Model of 1997 Dodge Caravan". NHTSA. Ashburn:, Virginia
- National Safety Council (NSC). (2018). (2017 Fatality Estimates) <http://www.nsc.org/learn/NSC-Initiatives/Pages/Fatality-Estimates.aspx>. [retrieved December 2018]
- Nevada Department of Public Safety. (2009). "Getting Ready to Drive. NV Driver Education Curriculum". USA: Nevada Department of Public Safety. Carson City, Nevada
- NHTSA. (2013). "Post-Crash Hydrogen Leakage Limits and Fire Safety Research". US DOT.
- NHTSA. (2014). "Evaluation of FMVSS No. 301". <https://crashstats.nhtsa.dot.gov/Api/Public/ViewPublication/812038>[retrieved December 2018]
- NHTSA. (2014). "Evaluation of FMVSS No. 301, Fuel System Integrity, as Upgraded in 2005 to 2009 ". US DOT, Washington DC:.
- NHTSA.(2016).*Crashstats-NHTSA-DOT*. <https://crashstats.nhtsa.dot.gov/#>[retrieved December 2018]
- NHTSA. (2018, October 29). Vehicle Database: Catalog Sorted by NHTSA Test Number. (NHTSA) <https://www-nrd.nhtsa.dot.gov/database/VSR/veh/VehicleCatalogTN.aspx>[retrieved December 2018]
- P.Siegmund, G., E.Heinrichs, B., D.Chimich, D., L.DeMarco, A., & R.Brault, J. (2005). "The Effect of Collision Pulse Properties on Seven Proposed Whiplash Injury Criteria". *Accident Analysis & Prevention*, 37(2), 275-285.
- Patel, D. V. (2007). "Study of rear impact in light trucks and potential injuries to the occupants". MS Thesis, Wichita State University, Wichita.
- Pennsylvania Department of Transportation. (2014). Pennsylvania Crash Facts & Statistics. Harrisburg: Bereau of Maintenance and Operations, Pennsylvania Department of Transportation.
- Pike. (1990). "Automotive Safety- Anatomy, Injury, Testing and Regulation".;Society of Automotive Engineers (SAE). Warrendale, PA.
- Prasad, P., & Daniel, R. P. (1984). "A biomechanical analysis of head, neck, and torso injuries to child". *28th Stapp Car Crash Conf.*.Chicago, IL.
- Ragland, C. L., & Hsia, H.-S. (1998). "'A Case Study of 214 Fatal Crashes Involving Fire". NHTSA, Ashburn, Virginia.

- Ranganatha, M. (2003). "Parametric Study of Neck Loads during Automobile Rear-end Impacts". MS Thesis, Wichita State University, Wichita.
- SAE. (1995). "Instrumentation for Impact Test-Part 1-Electronic Instrumentation". SAE. Warrendale, PA
- Schmitt et al. (2001). "A New Neck Injury Criterion Candidate for Rear-End Collisions Taking into Account Shear Forces and Bending Moments". Zurich, Switzerland.
- Sharon Tompkins. (2018). "What are the leading causes of rear-end collisions?" <https://www.lewisandtompkins.com/what-are-the-leading-causes-of-rear-end-collisions.html>[retrieved December 2018]
- SWOV. (1982). SWOV Institute for Road Safety Research, Netherlands.
- Tybout, Fahey, & Crowe. (14 August 2017). "Positioning the Tata Nano". Kellogg School of Management Cases, 1-12.
- US Department of Transportation. (1992). "Federal Aviation Regulation 25.562". Federal Aviation Administration.
- US Department of Transportation. (2007). "Laboratory Test Procedure For FMVSS 301R Fuel System Integrity- Rear Impact". NHTSA, Washington DC:
- Yoganandan, N. P., Pintar, F. A., & Kleinberger, M. P. (1999). "Whiplash Injury: Biomechanical Experimentation". *Spine*, 24(1), 83-85.